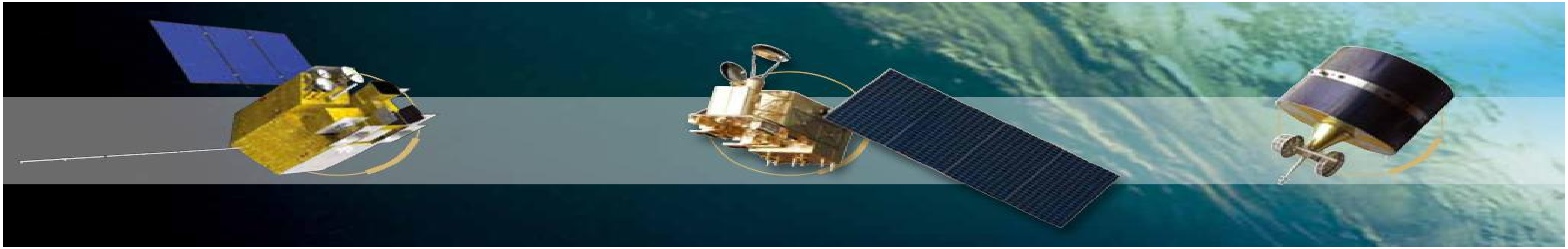

# 加速风云黎明星资料在数值预报同化系统中应用

翁富忠
中国气象局地球系统数值预报中心

2022年1月7日

# 中国气象局地球系统数值预报中心卫星资料同化室

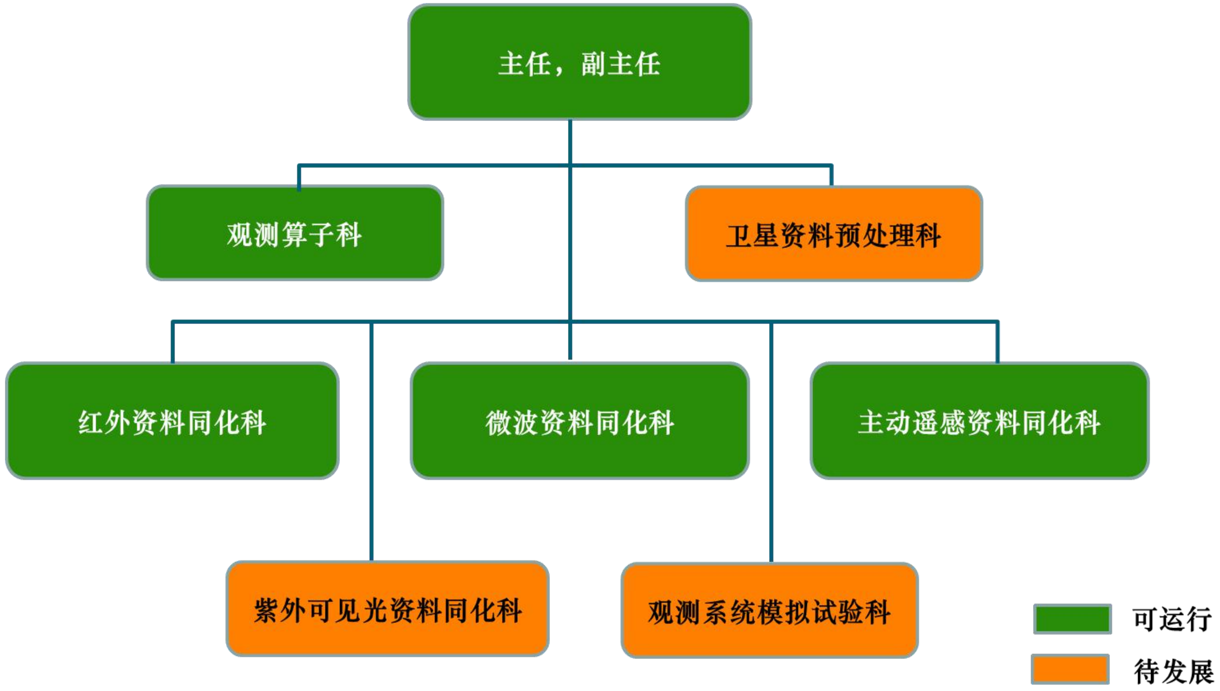


**Vision**: ***An organization working to become a national leader in applying satellite data and research to analysis and forecasting in CMA earth system numerical prediction models***

**Mission:** ***To accelerate and improve the quantitative use of research and operational satellite data in weather, ocean, climate and environmental analysis and prediction model***

# 中国气象局地球系统数值预报中心卫星资料科学优先级

- ***Satellite observation operators***
- ***Preparing for new instruments***
- ***Assimilation of cloud-affected radiances***
- ***Assimilation of land surface observations***
- ***Assimilation of ocean surface observations***
- ***Assimilation of air quality data***
- ***Observation system simulation experiments***

# 卫星观测算子和卫星资料同化关系

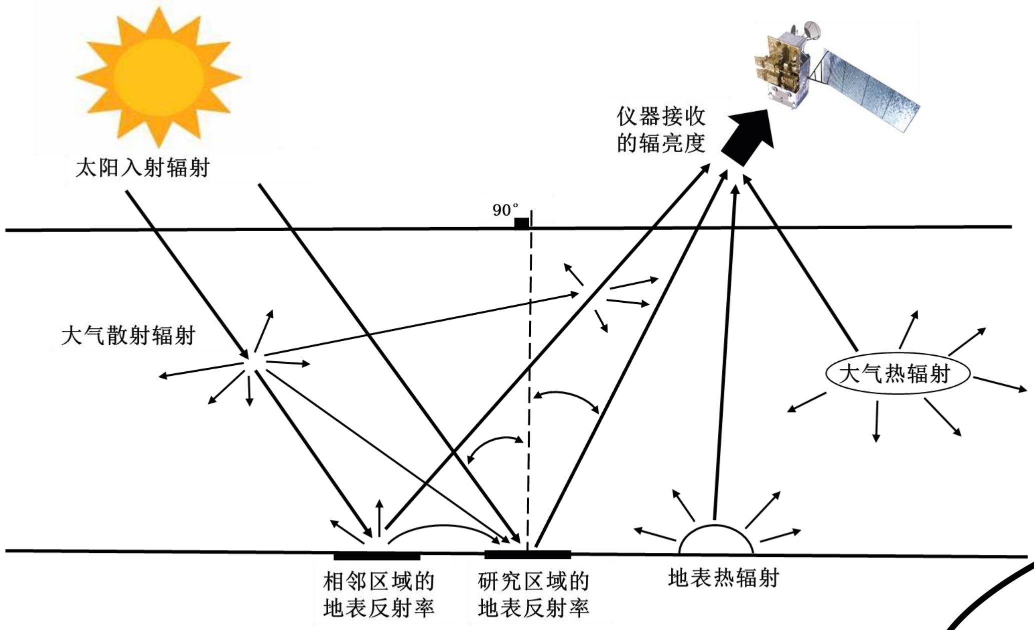


$$\mu\frac{d\mathbf{I}(\tau,\mu,\phi)}{d\tau}=-\mathbf{I}(\tau,\mu,\phi)+\frac{\omega(\tau)}{4\pi}\int_0^{2\pi}\int_{-1}^{1}\mathbf{M}(\tau,\mu,\phi;\mu',\phi')\mathbf{I}(\tau,\mu',\phi')d\mu'd\phi'+$$
$$+(1-\omega)B\begin{pmatrix}1\\0\\0\\0\end{pmatrix}+\frac{\omega F_0}{4\pi}\exp(-\tau/\mu_0)\begin{pmatrix}M_{11}(\phi,\mu_0,\phi_0)\\M_{12}(\phi,\mu_0,\phi_0)\\M_{13}(\phi,\mu_0,\phi_0)\\M_{14}(\phi,\mu_0,\phi_0)\end{pmatrix}$$

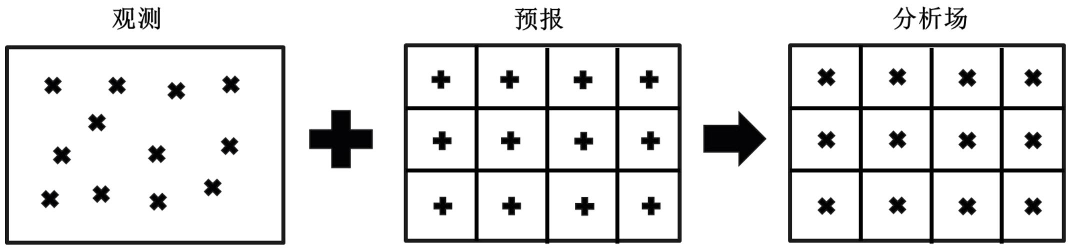


$$J(\mathbf{x})=\frac{1}{2}(\mathbf{x}-\mathbf{x}_b)^T\mathbf{B}^{-1}(\mathbf{x}-\mathbf{x}_b)+\frac{1}{2}(H(\mathbf{x})-\mathbf{y}^{obs})^T(\mathbf{O}+\mathbf{F})^{-1}(H(\mathbf{x})-\mathbf{y}^{obs})$$

$$J(\mathbf{x}_a)=\min_{\mathbf{x}}J(\mathbf{x})\quad\forall\mathbf{x}\text{ near }\mathbf{x}_b$$

$\mathbf{x}$ – analysis variable
$\mathbf{x}_a$ – final analysis
$\mathbf{x}_b$ – background
$\mathbf{B}$ – background error covariance
$\mathbf{y}^{obs}$ – observations
$\mathbf{O}$ – observation error covariance
$H$ – observation operator
$\mathbf{F}$ – forward model error covariance

卫星观测算子是使用辐射传输方程来描述光子在散射和吸收介质中的传输路径以及卫星仪器接收到的光子总量

资料同化的目的是利用不完整或不均匀的观测资料，给数值预报模式提供给定时间和指定分辨率的真实大气状态的一个比背景场更精确的估计——称做分析场

# 中国气象局快速辐射传输模式

# Advanced Radiative Transfer Modeling System (ARMS)

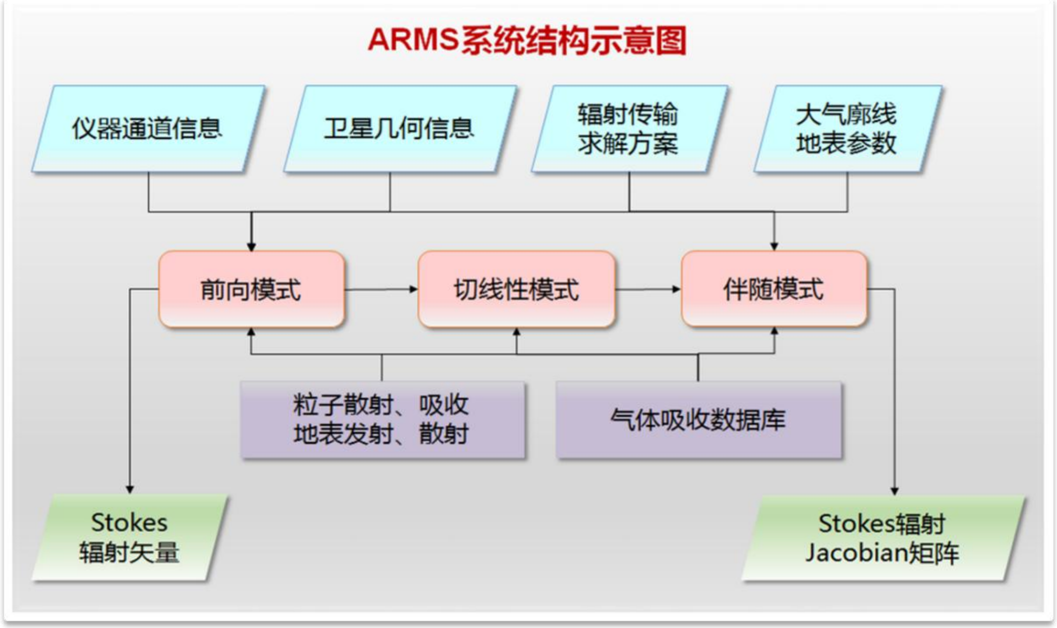


| 功能模块 | CRTM | RTTOV | ARMS |
|---|---|---|---|
| 辐射传输求解 | Advanced Doubling and Adding (ADA) | Delta-Eddington Approximation, DISORT, MFEAST | Polarization Two-Stream （P2S), HRTS, ADA, VDISORT |
| 散射特性 | Mie Table as a function of frequency, temperature, radii, and hydrometeor type and density | Mie Table as a function of frequency, temperature, and hydrometeor type and density, Discrete Dipole Approximation | Mie Table, T-Matrix as a function of frequency, temperature, and hydrometeor type and density. |
| 云类型 | Water, ice, rain, snow, graupel, hail | Water, ice, rain, and snow | Water, ice, rain, snow, graupel, hail |
| 地表模式 | NPOESS IR LUT, Wu/Smith IR Ocean EM, MW LandEM, FASTEM MW, Ocean EM | UWisc IR Emissivity Database, Cox/Munk IR Ocean EM, FASTEM, CNRW MW， TELSEM MW | Uwisc IR Emissivity Database, Wu/Smith IR Ocean EM, MW LandEM, FASTEM MW Ocean EM, AIEM, CNRW MW， TELSEM MW |

ARMS自2018年开始自主研发，现已通过中国气象局业务评审，与欧美的RTTOV和CRTM共同成为支撑卫星资料同化的核心支柱。

ARMS创新点：

- ✓ 采用全极化辐射求解方案
- ✓ 通用气溶胶云粒子散射计算理论与数据库
- ✓ 完善的海洋、陆面发射率理论模型和数据集
- ✓ 针对国产风云气象卫星仪器光谱特征的大气透过率快速计算模型

# 快速辐射传输模式(ARMS)主要用户

| ARMS主要用户 | 应用场景 |
| --- | --- |
| 数值中心 | 全球、区域卫星资料同化 |
| 气象中心 | 卫星微波反演大气廓线台风定强定位 |
| 信息中心 | 全球再分析同化及质量融合 |
| 南京气象创新院 | 风云卫星红外高光谱反演系统 |
| 上海台风所 | 华东区域模式同化系统 |
| 大湾区预报中心 | 华南区域模式同化系统 |
| 卫星中心 | 卫星仿真模拟系统 |
| 美国NOAA | 风云卫星资料同化 |
| 美国卫星资料同化中心 | 风云卫星资料同化 |
| 气科院 | 仪器在轨测试、卫星遥感应用 |
| 国防科大 | 卫星资料同化与应用 |
| 北京大学 | 全球降水反演与融合 |

# ARMS 支撑的国内外仪器

- NOAA 15 to 19 AMSU-A
- NOAA 18-19 MHS
- NOAA 18-19 HIRS
- NOAA 15-19 AVHRR
- SNPP/NOAA-20 ATMS
- SNPP/NOAA-20 CrIS
- SNPP/NOAA-20 VIIRS
- METOP-A to C IASI
- METOP-A to C IASI
- METOP-A to C AMSU-A
- METOP-A to C AVHRR
- JAXA AMSR2
- NASA GMI
- EOS Aqua AIRS
- EOS Terra/Aqua MODIS

- FY-3A MWTS
- FY-3A MWHS
- FY-3B MWTS
- FY-3B MWHS
- FY-3C MWTS-2
- FY-3C-MWHS-2
- FY-3D MWTS-2
- FY-3D MWHS-2
- FY-3B/C/D MWRI
- FY-3B/C VIRR
- FY-3C MERSI
- FY-3C IRAS
- FY-3D MERSI-2
- FY-3D HIRAS
- FY-4A GIIRS
- FY-4A AGRI

- FY-3E MWTS
- FY-3E MWHS
- FY-3E HIRAS-2
- FY-3E MERSI-LL
- FY-3E Windrad
- FY-3E GNOS-R
- FY-4B GIIRS
- FY-4B AGRI
- FY-4B GHI
- FY-4M GMIS

# 快速辐射传输模式(ARMS)在数值预报同化及遥感中应用

1. **ARMS的主要研发进展**：1）基于海洋双尺度粗造度功率谱的全极化反射率模型 2）新增两种辐射传输求解方案。

2. **ARMS的主要NWP用户**：中国气象局数值中心、解放军国防科技大学、NOAA卫星资料同化联合中心等10多家单位，在台风模式在 应用效果明显(见右图）。

3. **ARMS 在反演系统中应用**：用于风云卫星全球反演大气温湿度廓线。效果优于美国的CRTM（见下图）

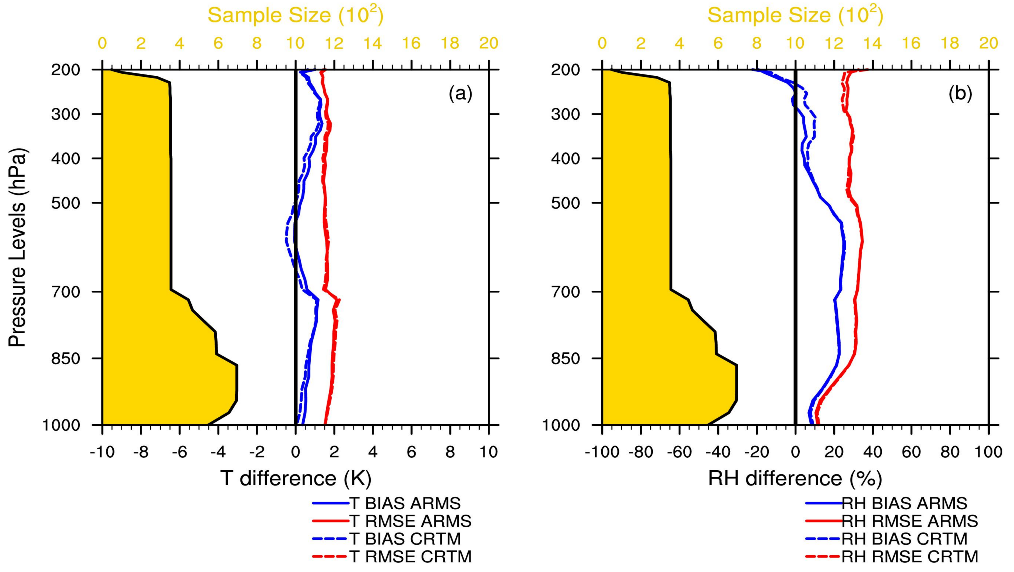


## 台风利奇马路径预报误差统计

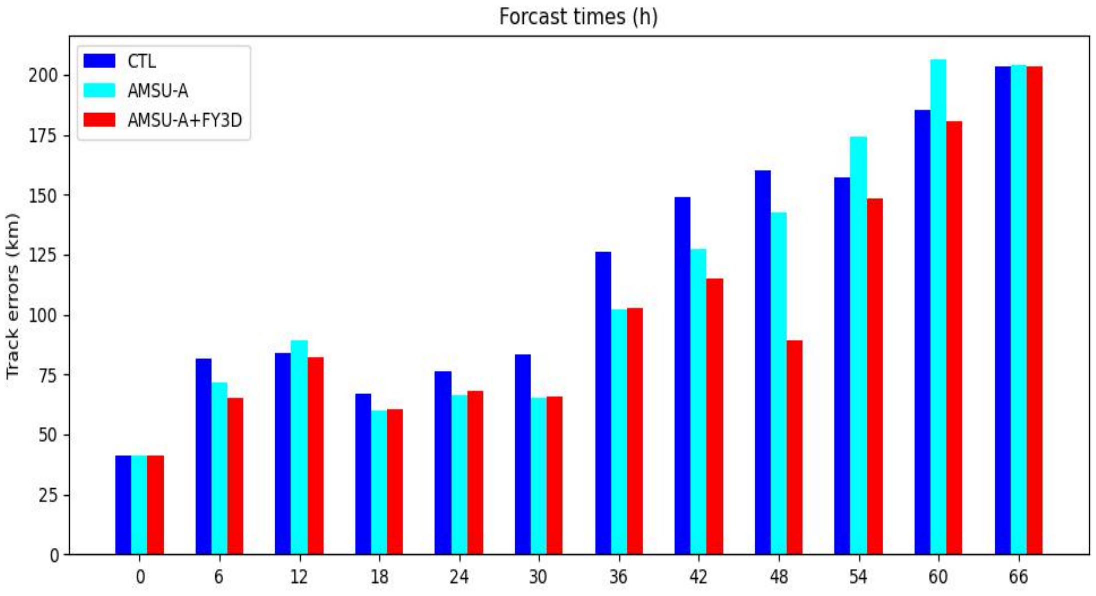


- 上海台风研究所在区域模式中引入ARMS替代原同化系统中的美国研发的CRTM。
- 由于使用ARMS，实现了风云卫星微波资料数据在上海区域模式同化应用
- 从4个起报时次的路径预报误差统计分析结果看，同化风云卫星资料（AMSU+FY-3D）对改进台风利奇马路径预报表现为正效果，在66h预报时效内平均误差都是有明显降低

# 中国气象卫星发展计划特色

## 风云四号特色

- GIIRS： 静止红外大气探测干涉仪
- GMAS：静止微波大气探测仪
- Space Weather Instruments

## 风云三号特色

- MWTS/MWHS: 双氧探测通道, 共32 个通道
- MERSI-LL: 微光成像仪
- PR: 降水雷达
- GNOS-R：掩星海洋反射计测风
- Space Weather Instruments

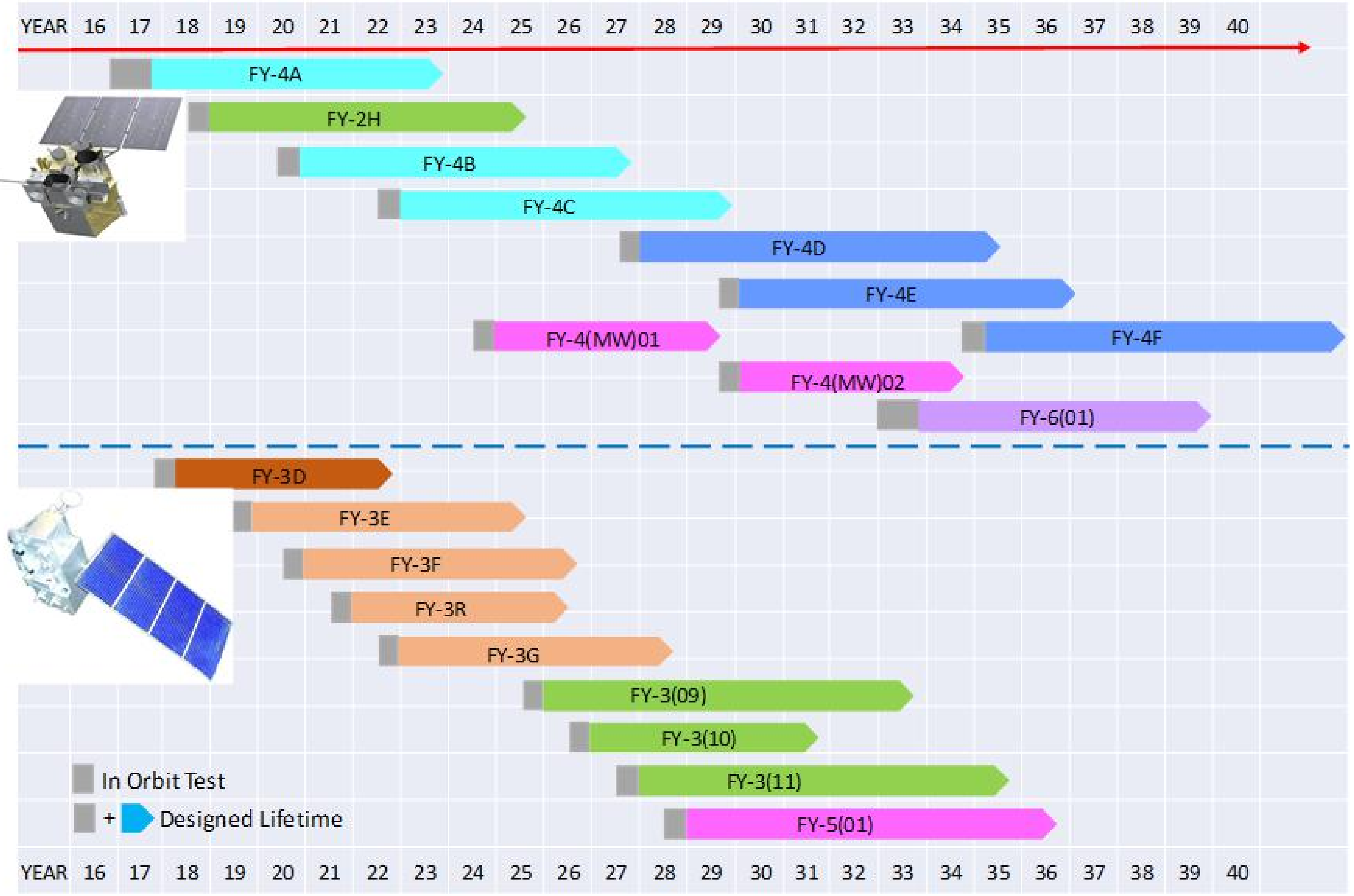

# FengYun (FY)-3E Early Morning Satellite

- The CMA first operational weather satellite launched on July 5, 2021 in the early morning orbit at 5:40 am local time
- It carries 13 payloads onboard and constellates with NOAA and EUMETSAT weather satellites

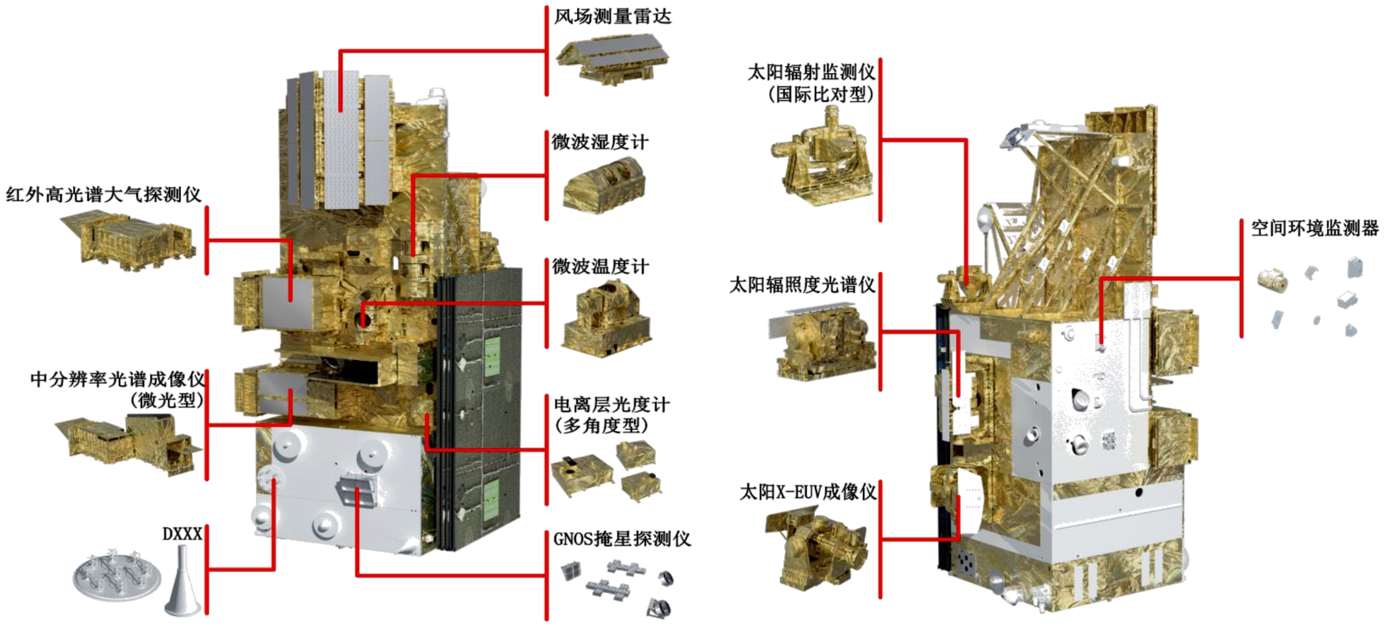


| Acronym | Full name |
|---|---|
| MWHS-2 | Micro-Wave Humidity Sounder -2 |
| SIM-2 | Solar Irradiance Monitor - 2 |
| WindRAD | Wind Radar |
| SWS/SEM/HEPD | Space Weather Suite / Space Environment Monitor / High Energy Particle Detector |
| SWS/SEM/IMS | Space Weather Suite / Space Environment Monitor / Ionosphere Measurement Sensor |
| SWS/Tri-IPM | Space Weather Suite - Triple-angle Ionospheric PhotoMeter |
| XEUVI | Solar X-ray and Extreme Ultraviolet Imager |
| MWTS-3 | Micro-Wave Temperature Sounder - 3 |
| HIRAS-2 | Hyperspectral Infrared Atmospheric Sounder - 2 |
| MERSI-LL | Medium Resolution Spectral Imager - Low-Light |
| SSIM | Solar Spectral Irradiance Monitor |
| SWS/SEM/MFD | Space Weather Suite / Space Environment Monitor / Magnetic Field Detector |
| GNOS-2 | GNSS Radio Occultation Sounder - 2 |

# ARMS 模拟FY-3E MWTS-3/MWHS-2 精度

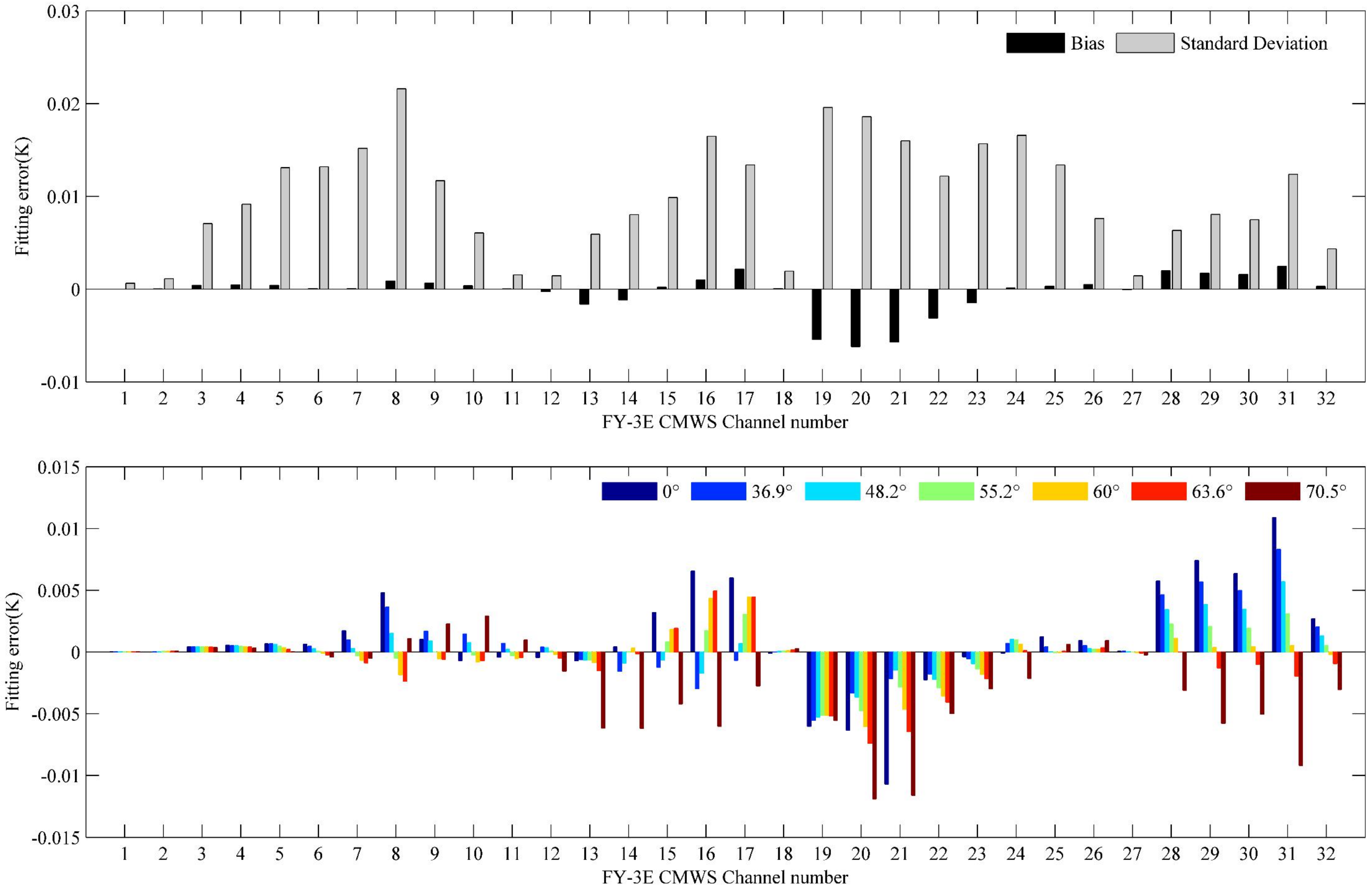

# ARMS 模拟FY-3E HIRAS-2 精度

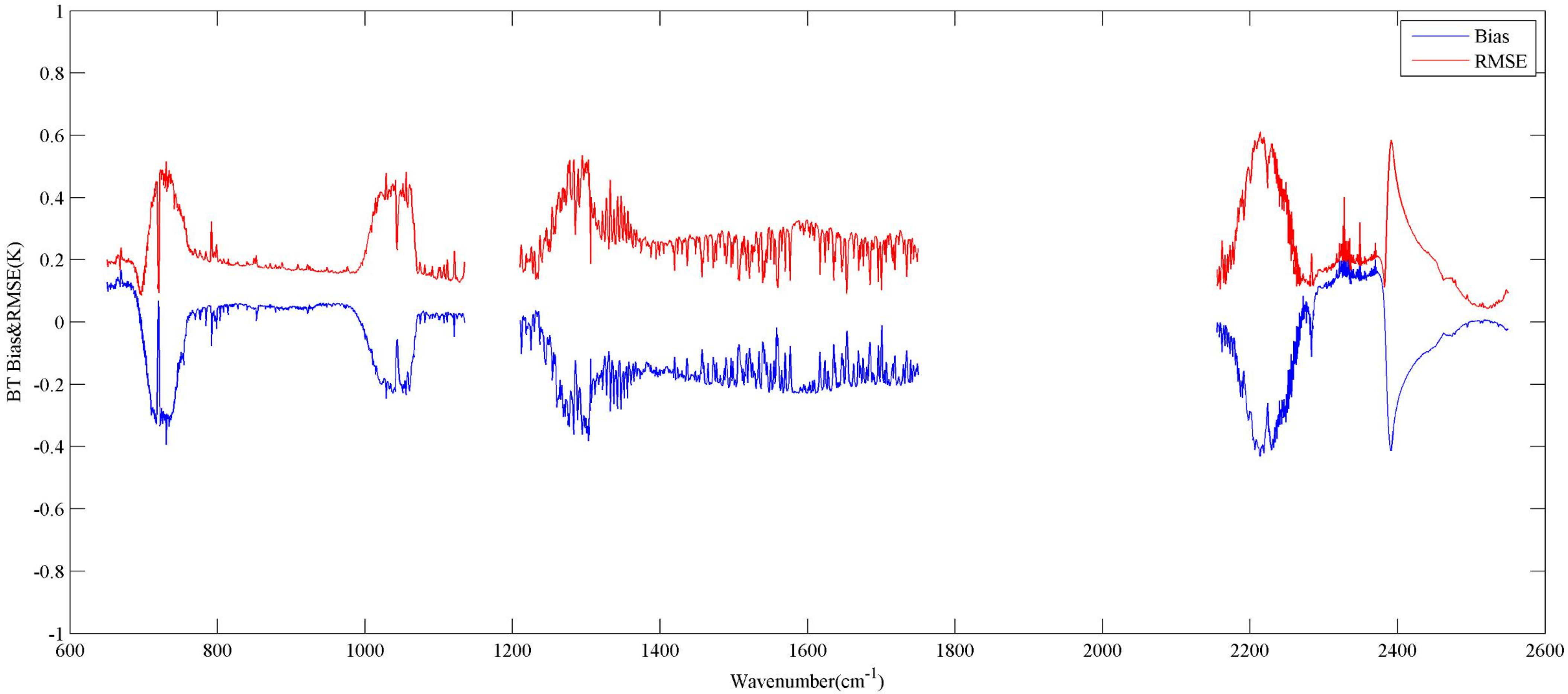

# Micro-Wave Temperature Sounder (MWTS)- 3

**23.8 GHz**

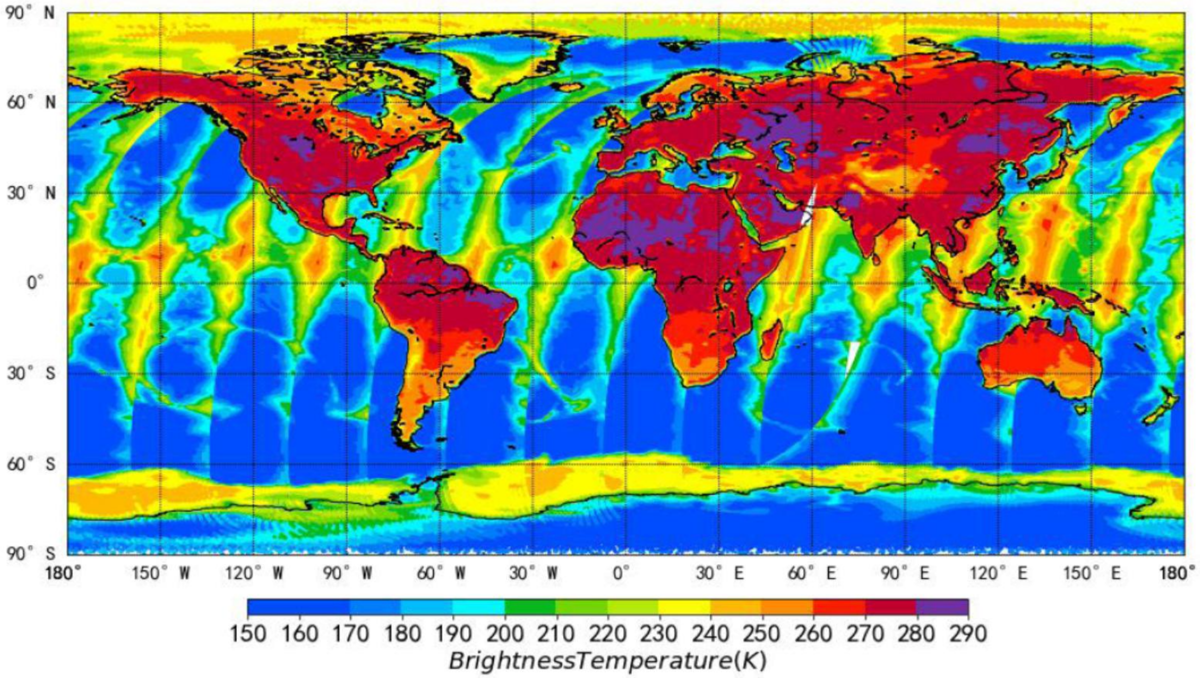


**31.4 GHz**

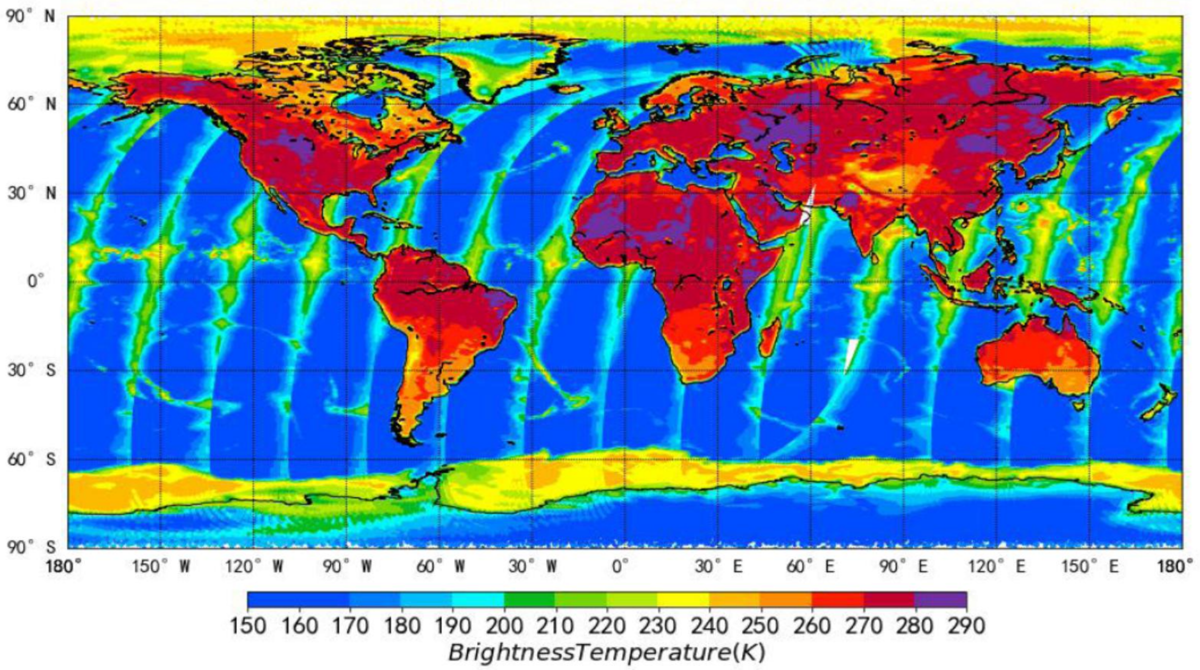


*MWTS-3 two newly added K/Ka bands at 23.8 and 31.4 GHz provide nice surface characteristics. The observations from open waters are largely dominated by the scan angle dependence. Overall, there is no orbit gaps due to an increase of scan swath of MWTS-3 with respect to MWTS-2*

# Characteristics of MWTS-3 Polarization Alignment

https://space.oscar.wmo.int/satellites/view/fy_3e

MWTS-3

| Ch | Frequency (GHz) | Bandwidth (MHz) | Polarization | Spatial Resolution (km) | Applications |
|---|---|---|---|---|---|
| 1 | 23.8 | 270 | V or H | 50 | Water vapor, clouds, surface emissivity |
| 2 | 31.4 | 180 | V or H | 50 | Water vapor, clouds, surface emissivity |
| 3 | 50.3 | 180 | V or H | 33 | Atmospheric temperature profile |
| 4 | 51.76 | 400 | | 33 | |
| 5 | 52.8 | 400 | | 33 | |
| 6 | 53.246±0.08 | 2*140 | | 33 | |
| 7 | 53.596±0.115 | 2*170 | | 33 | |
| 8 | 53.948±0.081 | 2*142 | | 33 | |
| 9 | 54.40 | 400 | | 33 | |
| 10 | 54.94 | 400 | | 33 | |
| 11 | 55.50 | 330 | | 33 | |
| 12 | 57.290344(fo) | 330 | | 33 | |
| 13 | fo±0.217 | 2*78 | | 33 | |
| 14 | fo±0.3222±0.048 | 4*36 | | 33 | |
| 15 | fo±0.3222±0.022 | 4*16 | | 33 | |
| 16 | fo±0.3222±0.010 | 4*8 | | 33 | |
| 17 | fo±0.3222±0.0045 | 4*3 | | 33 | |

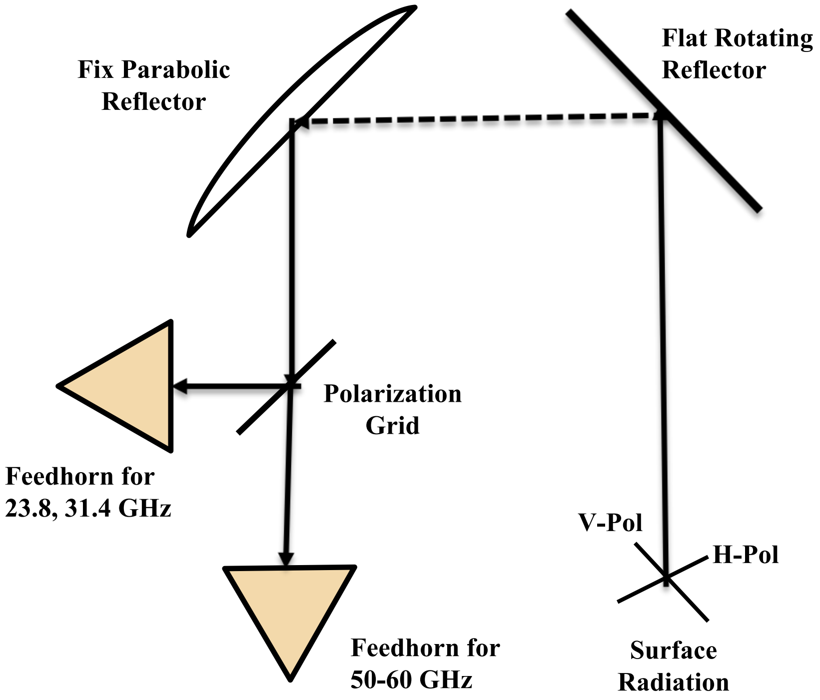


$$\begin{bmatrix} T_B^{QV} \\ T_B^{QH} \\ T_B^{Q3} \\ T_B^{Q4} \end{bmatrix} = \begin{bmatrix} \cos^2\theta & \sin^2\theta & 0.5\sin 2\theta & 0 \\ \sin^2\theta & \cos^2\theta & -0.5\sin 2\theta & 0 \\ -\sin 2\theta & \sin 2\theta & \cos 2\theta & 0 \\ 0 & 0 & 0 & 1 \end{bmatrix} \begin{bmatrix} T_B^{V} \\ T_B^{H} \\ T_B^{3} \\ T_B^{4} \end{bmatrix}$$

**MWTS-3 New Channels: 23.8, 31.4, 53.596 ± 0.115 and 53.948 ± 0.081 GHz; New Scan Pattern: Cross-track: 98 FOV, Sync with MWHS-2; Uniformly scan; Scan Swath: 2700 km; Coverage / Cycle: Near-global coverage twice/day. Polarization for MWTS-3 is uncertain.**

# MWTS-3 K/Ka 波段 极化特性研究

**Methodology:**

- Simulate MWTS with NCEP analysis data as inputs to radiative transfer models
- Compute MWTS observations minus simulations (O-B) in clear-sky ocean conditions
- MWTS brightness temperatures are simulated with either vertical or horizontal polarization
- Cloud-affected MWTS observations are removed through uses of FY-4A AGRI data
- MWTS O-B is also compared with ATMS O-B as well as ATMS pitch maneuver observations

**Tools and Datasets:**

- Radiative transfer models: Advanced Radiative Transfer Modeling System (ARMS 1.1.1)
- NCEP Global Analysis Data: July 12 to August 10, 2021
- Satellite Data: FY-3E MWTS-3, Suomi NPP ATMS, FY-4A AGRI

**Quasi-Vertical Polarization**

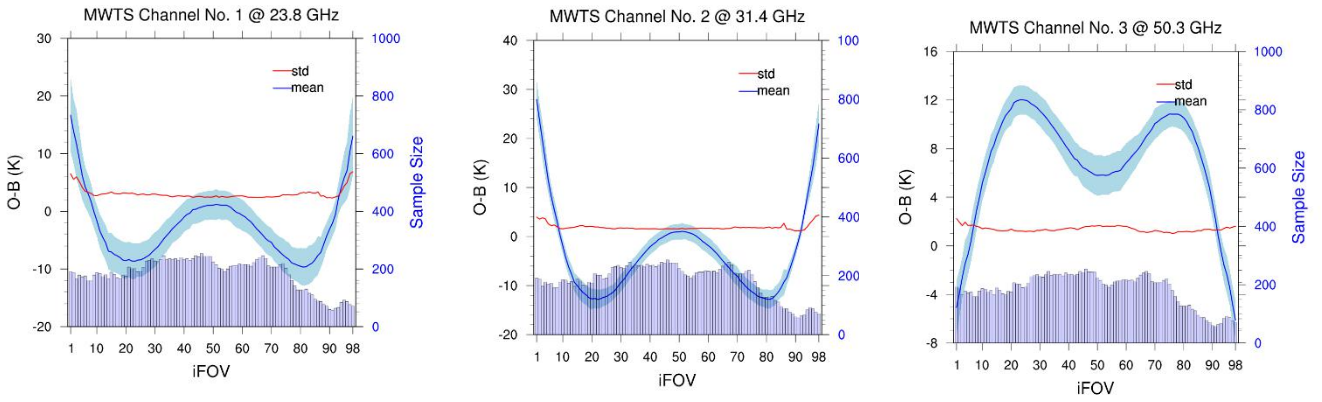


**Quasi-Horizontal Polarization**

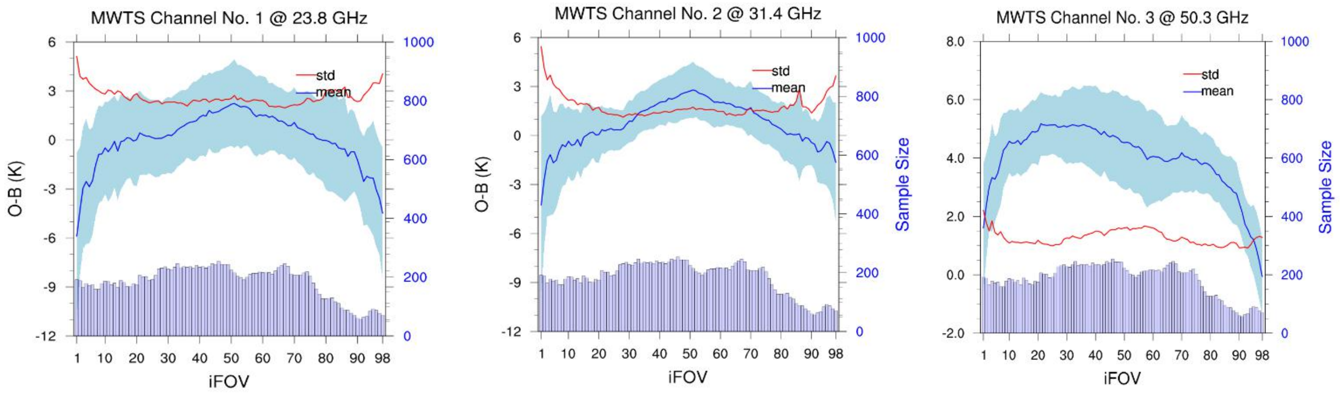


阚婉琳，董嫦娇

# MWTS-3 与ATMS 极化特性比较

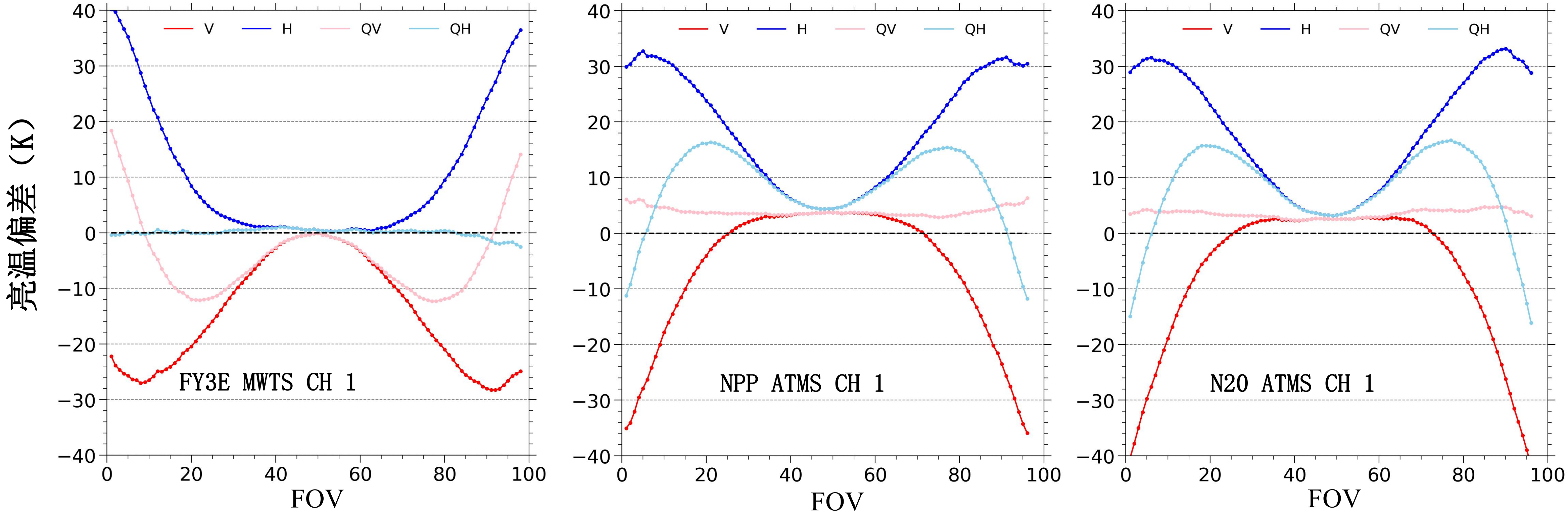


2021年7月5日发射的FY-3E卫星搭载的MWTS增加了23.8、31.4GHz等4个通道，为云水反演和仪器资料同化云检测提供了重要观测资料。

- 输入ERA5再分析资料到ARMS模式中，模拟计算出FY-3E卫星MWTS的不同极化方式耦合方案的亮温，比较观测和模拟亮温在不同角度上的偏差。
- 通过在轨测试实验发现通道1（21.8GHz）、通道2（31.4 GHz）、通道3（50.3 GHz）观测亮温与极化方式分别是基于准水平、准水平和准垂直极化的模拟亮温偏差更小，与ATMS极化方式相反。

韩阳

# Cloud Liquid Water Algorithm

$$\kappa_V V + \kappa_L L = -\frac{\mu}{2}\left\{\ln(T_s - T_b) - \ln[T_s(1-\epsilon)] + \frac{2\tau_{O_2}}{\mu}\right\} \quad (6.12)$$

Using two channel measurements, we can derive

$$L = a_0\mu[\ln(T_s - T_{b,1}) - a_1 \ln(T_s - T_{b,2}) - a_2], \quad (6.13)$$

and

$$V = b_0\mu[\ln(T_s - T_{b,1}) - b_1 \ln(T_s - T_{b,2}) - b_2], \quad (6.14)$$

respectively. $T_{b,1}$ is the channel sensitive to liquid and $T_{b,2}$ is the channel sensitive to water vapor. The coefficients, $a_{0,1,2}$ and $b_{0,1,2}$ are related to water vapor and liquid water mass absorption coefficients as

$$a_0 = -0.5\kappa_{V2}/(\kappa_{V2}\kappa_{L1} - \kappa_{V1}\kappa_{L2}) \quad (6.15)$$

$$b_0 = 0.5\kappa_{L2}/(\kappa_{V2}\kappa_{L1} - \kappa_{V1}\kappa_{L2}) \quad (6.16)$$

$$a_1 = \kappa_{V1}/\kappa_{V2} \quad (6.17)$$

$$b_1 = \kappa_{L1}/\kappa_{L2} \quad (6.18)$$

$$a_2 = -2(\tau_{O,1} - a_1\tau_{O,2})/\mu + (1-a_1)\ln[T_s(1-\epsilon_1)] - a_1\ln(1-\epsilon_2) \quad (6.19)$$

$$b_2 = -2(\tau_{O,1} - b_1\tau_{O,2})/\mu + (1-b_1)\ln[T_s(1-\epsilon_1)] - b_1\ln(1-\epsilon_2) \quad (6.20)$$

From Rayleigh's approximation, $\kappa_L$ can be parameterized as a function of cloud layer temperature, $T_L$ in Celsius as

$$\kappa_L = a_L + b_L T_L + C_L T_L^2, \quad (6.21)$$

Oxygen optical thickness is parameterized as a function of sea surface temperature through

$$\tau_O = a_o + b_o T_s, \quad (6.22)$$

Table 6.1: The parameters calculated at four AMSU-A channels and used in liquid water and water vapor path algorithms

| | 23.8 GHz | 31.4 GHz | 50.3 GHz | 89 GHz |
|---|---|---|---|---|
| $\kappa_V$ | 4.80423E-3 | 1.93241E-3 | 3.76950E-3 | 1.15839E-2 |
| $\kappa_L$ - $a_L$ | 1.18201E-1 | 1.98774E-1 | 4.53967E-3 | 1.03486E00 |
| $\kappa_L$ - $b_L$ | -3.48761E-3 | -5.45692E-3 | -9.68548E-3 | -9.71510E-3 |
| $\kappa_L$ - $c_L$ | 5.01301E-5 | 7.18339E-5 | 8.57815E-5 | -6.59140E-5 |
| $\tau_O$-$a_o$ | 3.21410E-2 | 5.34214E-2 | 6.26545E-1 | 1.08333E-1 |
| $\tau_O$-$b_o$ | -6.31860E-5 | -1.04835E-4 | -1.09961E-3 | -2.21042E-4 |

# 风云卫星FY-3E(黎明星）与NOAA 微波大气探测全球云液态水分布对比

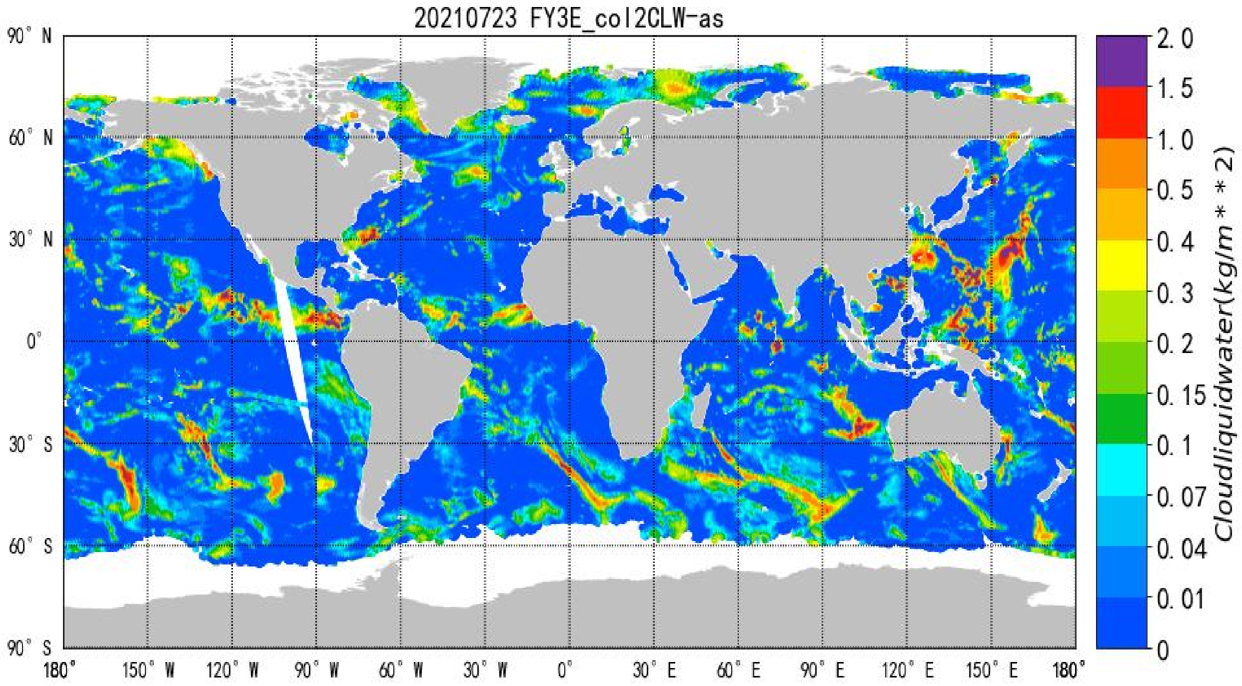


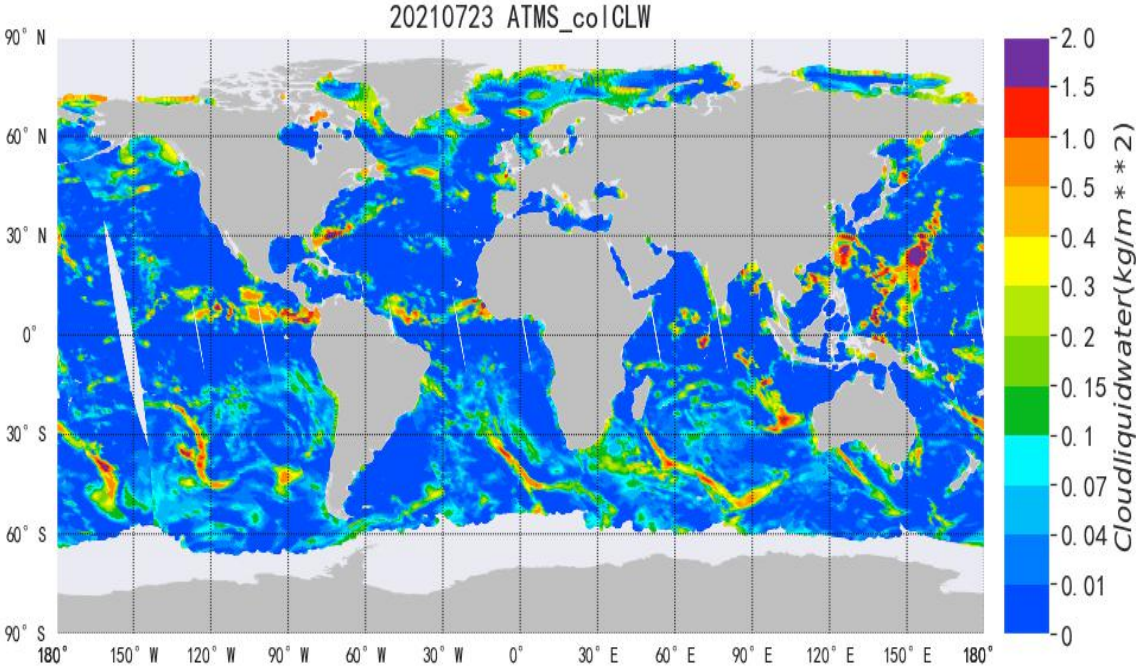


*Cloud liquid water retrieved from MWTS Channel 1 and 2 is consistent with ATMS's clouds. However, since Suomi NPP and FY-3E are flying in different orbits, the spatial difference is more related to the diurnal variation of clouds and precipitation observed from two instruments.*

# FY-3E MWTS/MWHS 与NOAA ATMS O-B 对比

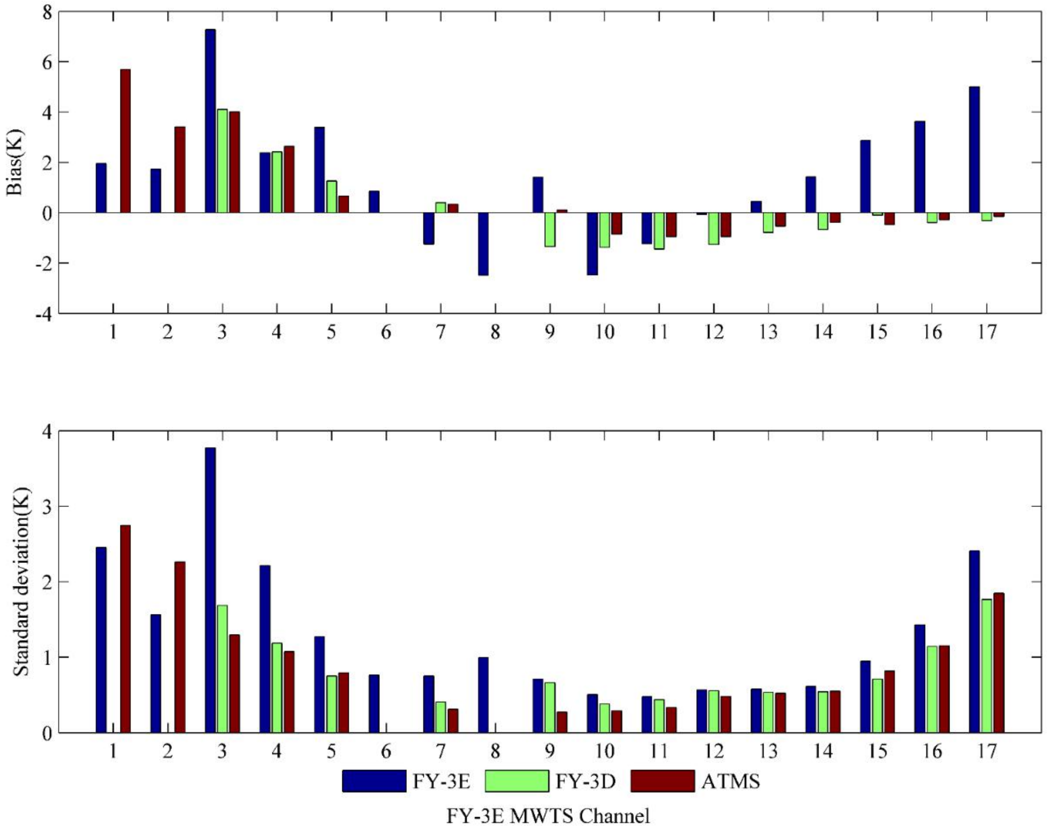


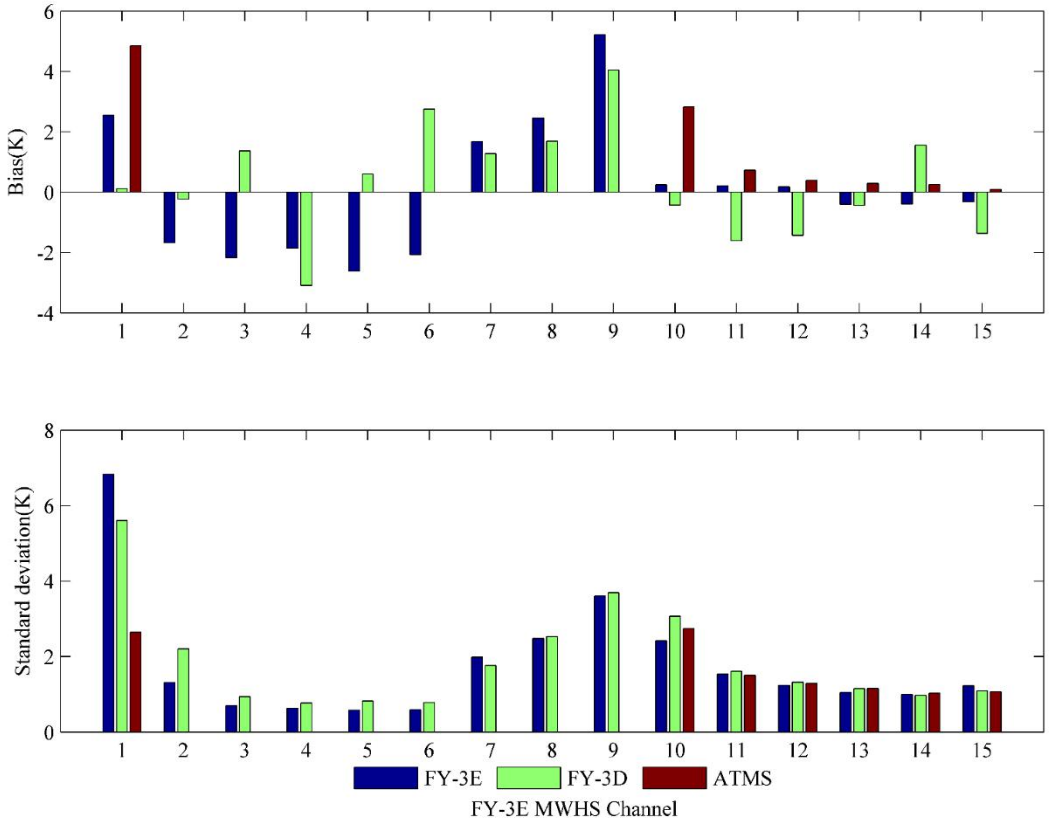


2021.7.11-8.9 30天　GFS 40层廓线
AGRI云产品匹配做云检测＆风速<5m/s　洋面

阚婉琳等，2022

# FY-3E MWTS/MWHS 升、降轨差异 评估

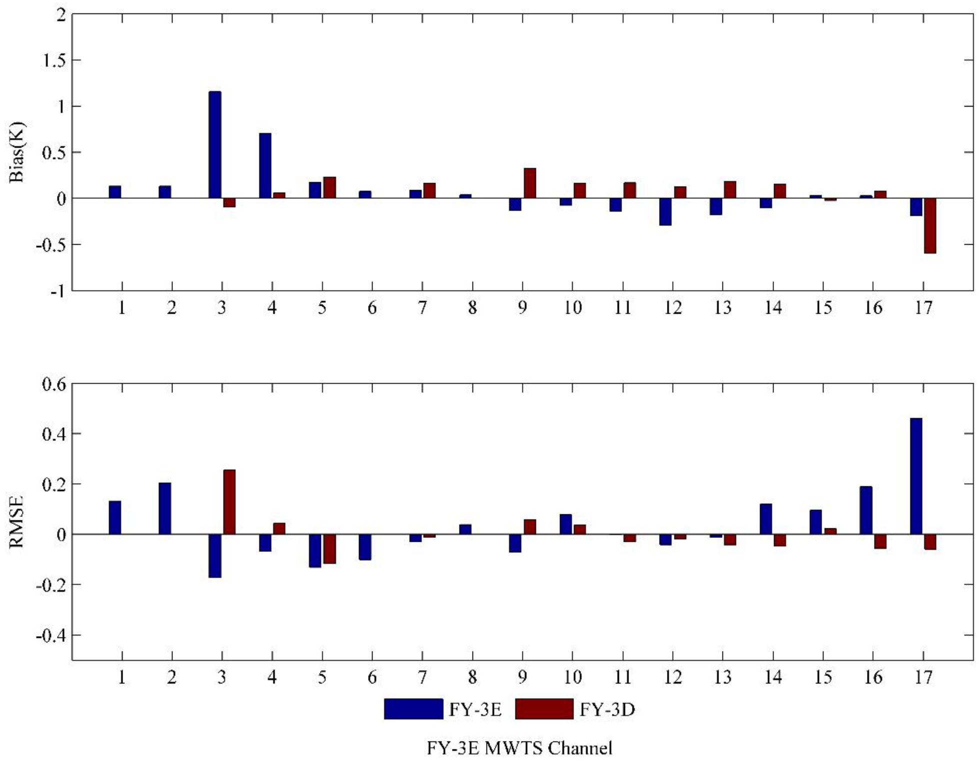


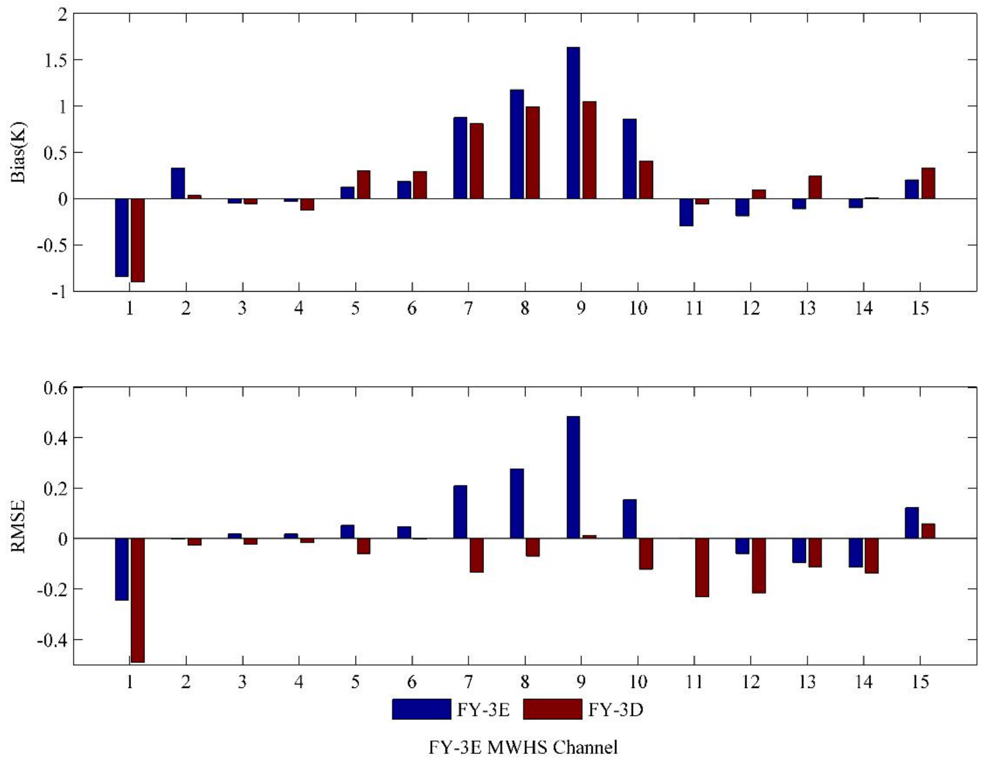


2021.7.11-8.9 30天　GFS 40层廓线
AGRI云产品匹配做云检测＆风速<5m/s　洋面

阚婉琳等，2022

# FY-3E MWTS/MWHS 条纹噪声指数(Striping Index)

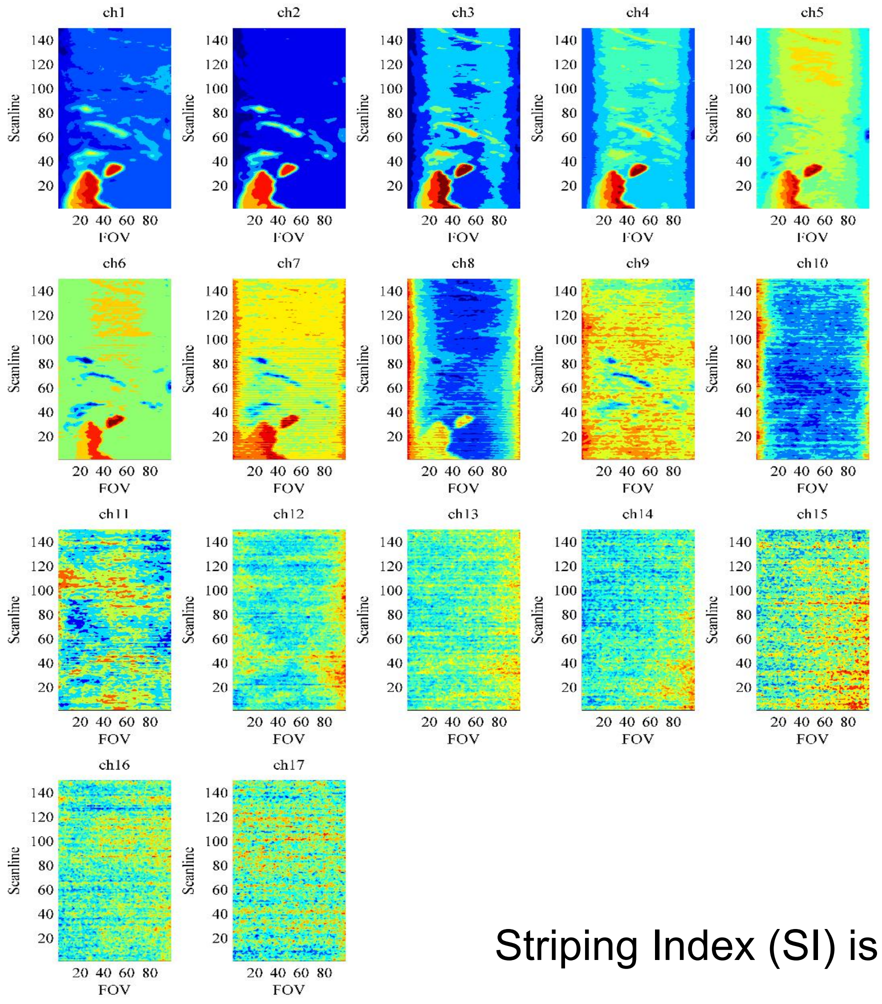


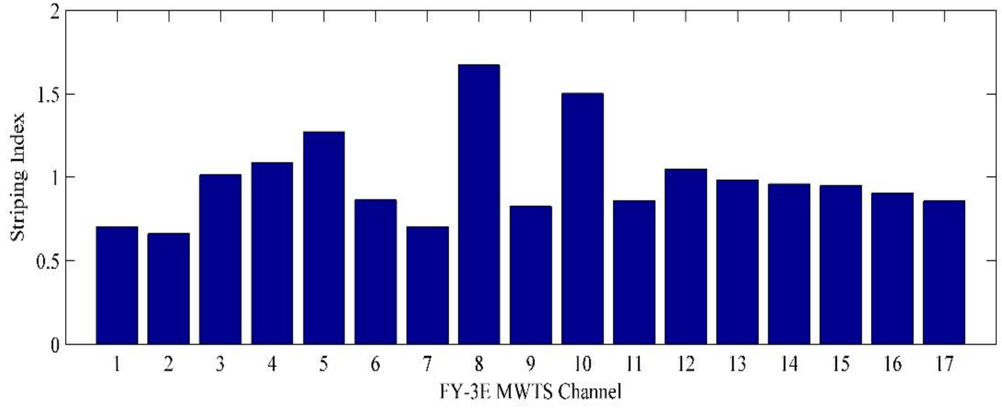


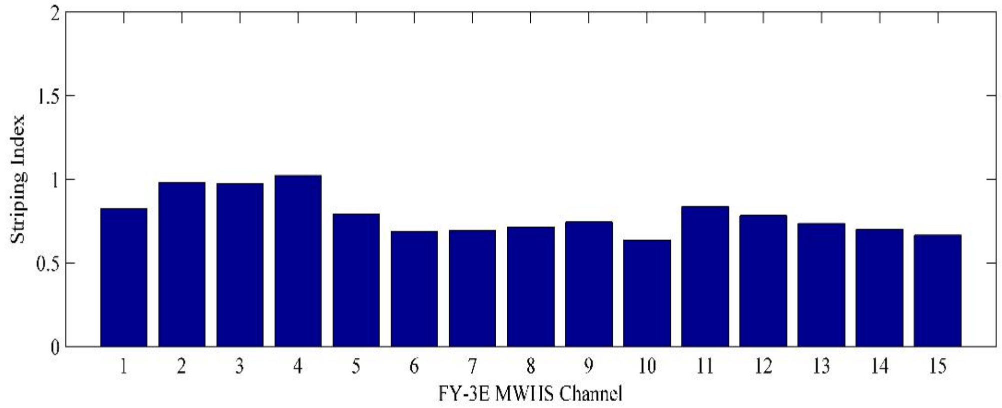


Striping Index (SI) is defined as a ratio of cross-track noise to the along-track noise

阚婉琳等, 2022

# FY-3E 微波探测资料在CMA_GFS同化产生正效应

20210924-1009分析场（南/北半球分析误差降低）

FY-3E MWTS-3反演云水

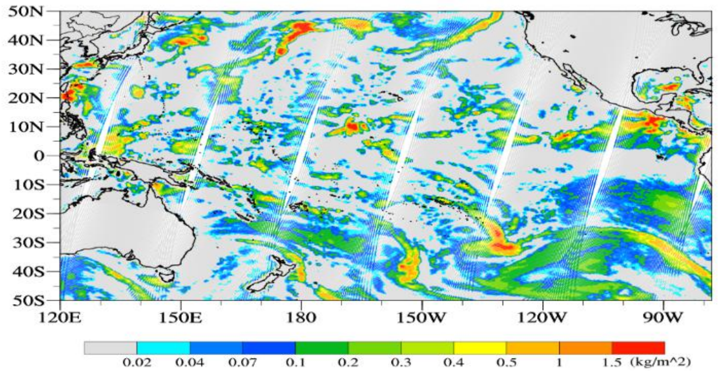

ERA5云水产品

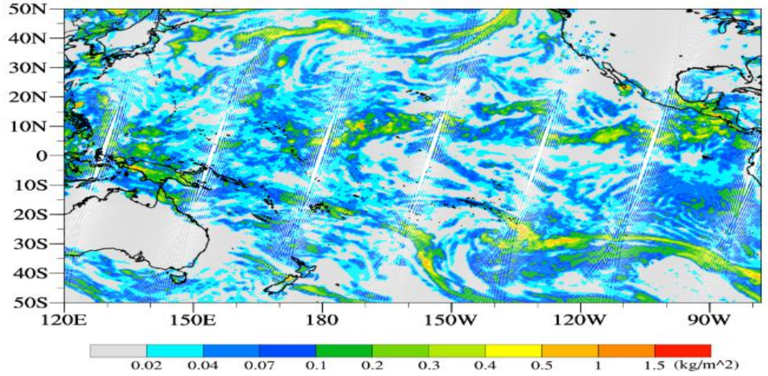

李娟等, 2021

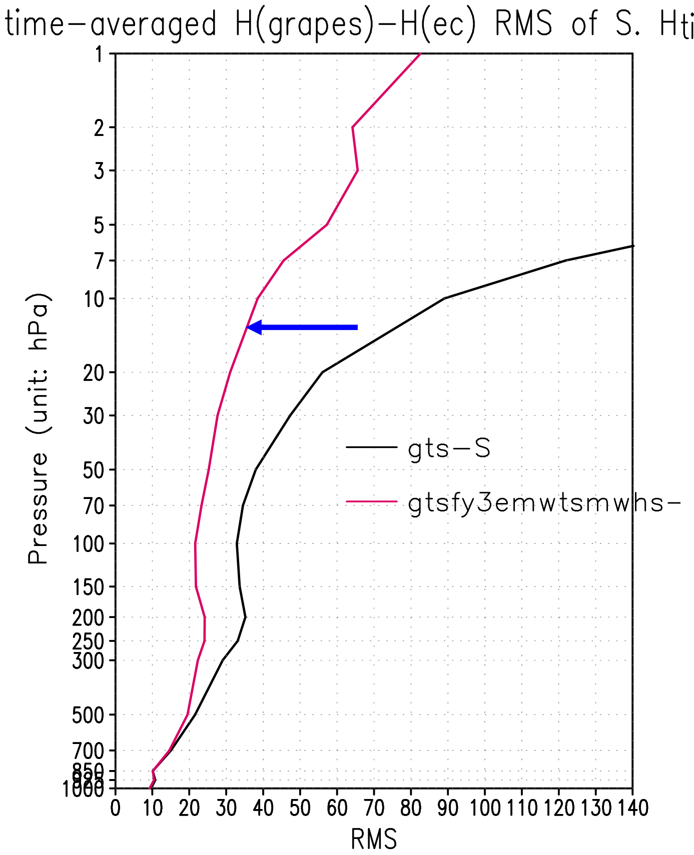


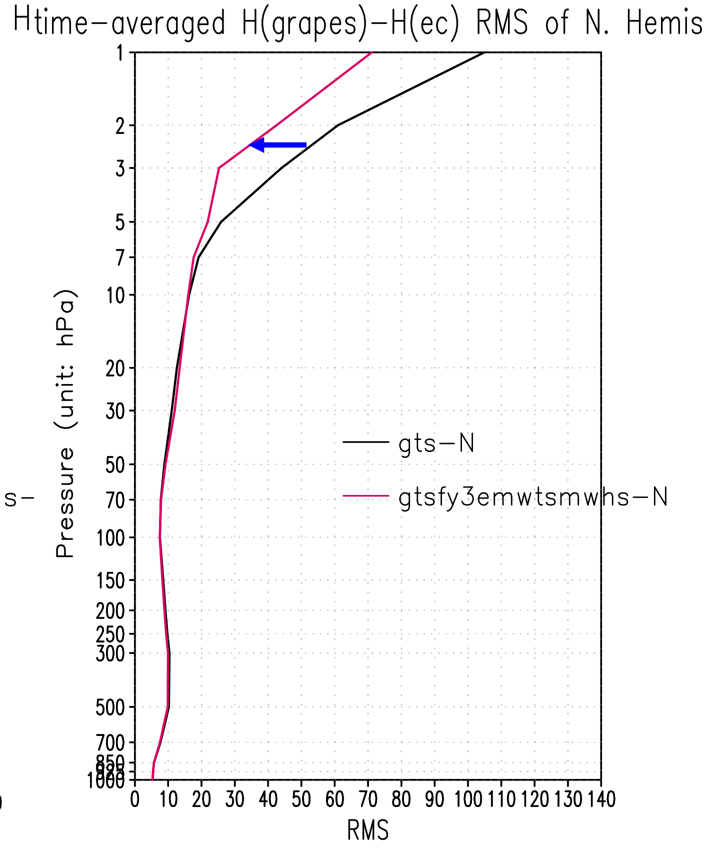


李娟，刘桂青等

在常规资料基础上增加FY-3E微波温度计/湿度计，显著正效果

# FY-3E 微波探测资料在CMA_GFS同化正效应在南半球更明显

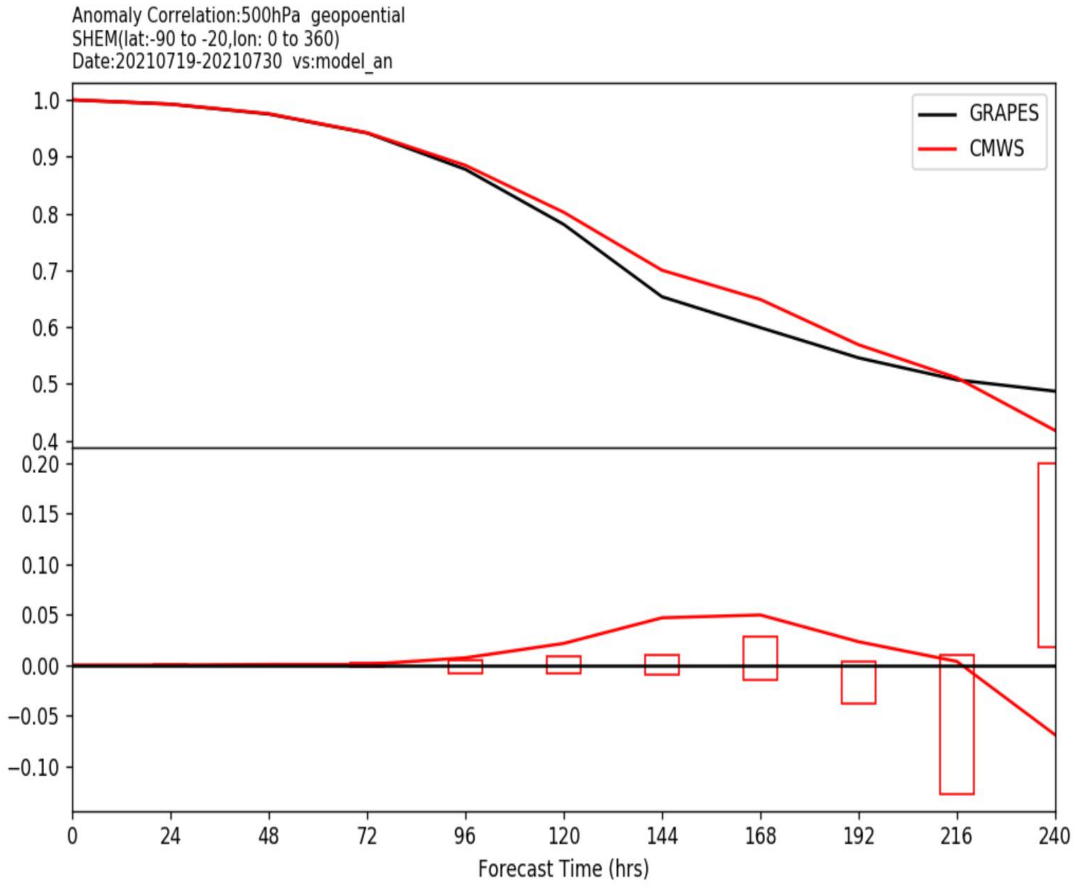


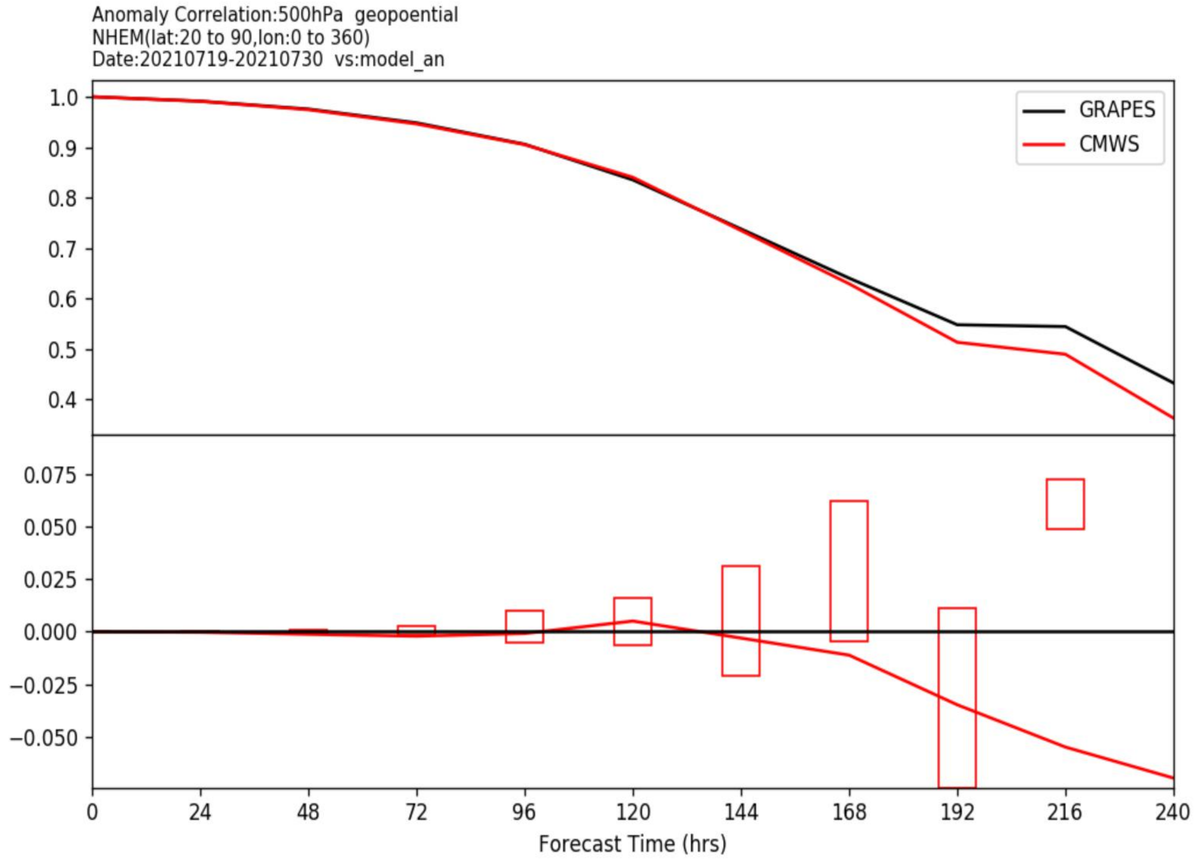

# 全球场景自适应微波集成反演系统

**Global Scene-Dependent Atmospheric Retrieval Testbed(GSDART)**

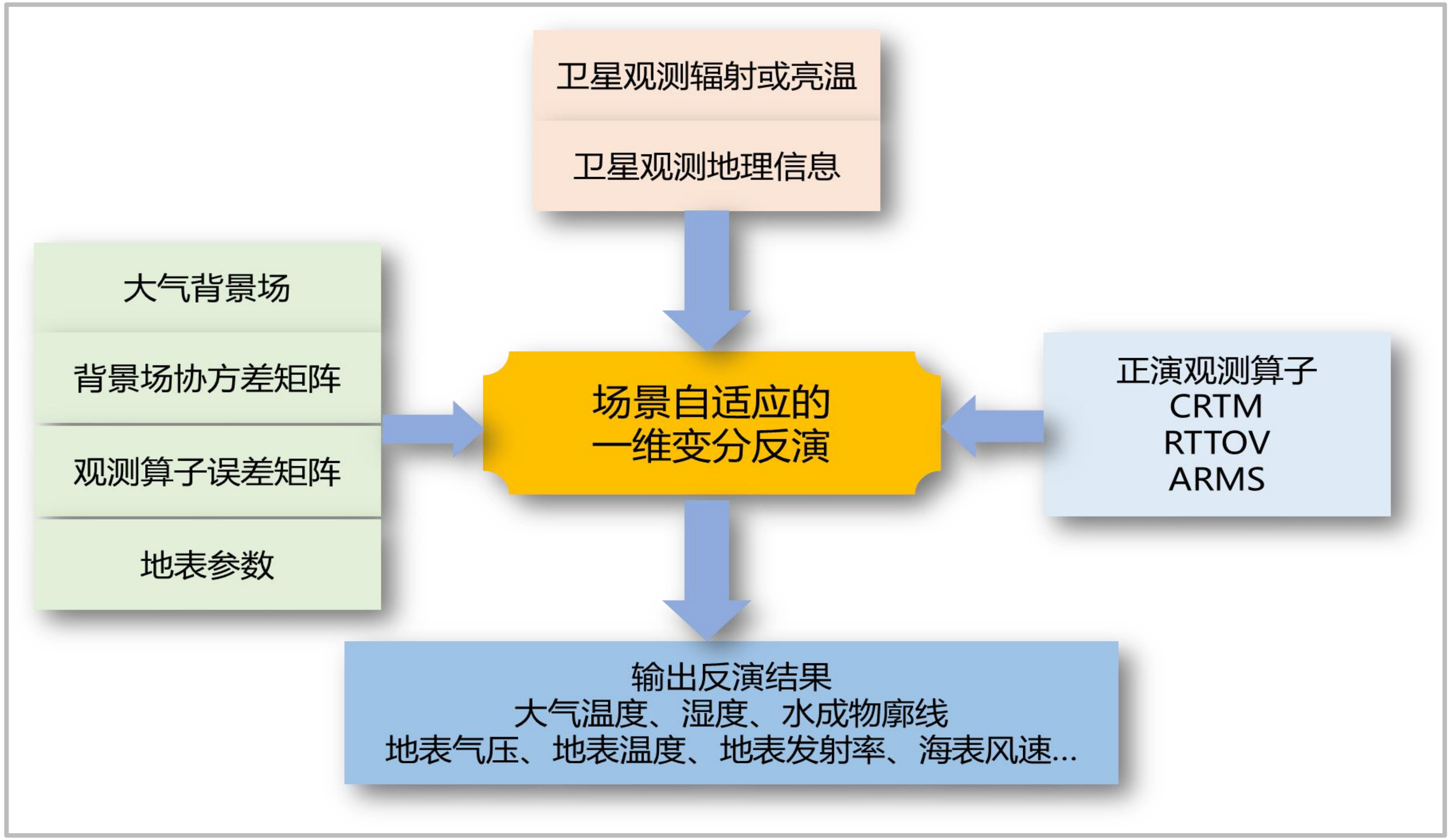


胡皓

- Work for all the microwave instruments
- Work under all the conditions
- Advanced retrieval sciences
- Simultaneous retrievals of a suite of parameters
- Powerful post-processing

| |
|---|
| Temperature profile |
| Moisture profile |
| Total precipitable water |
| Hydrological profile |
| Precipitation rate |
| Snow cover |
| Snow water equivalent |
| Sea ice concentration |
| Cloud water path |
| Ice water path |
| Surface temperature |
| Surface emissivity |
| Wetness index |

# 耦合静力积分反演海平面气压

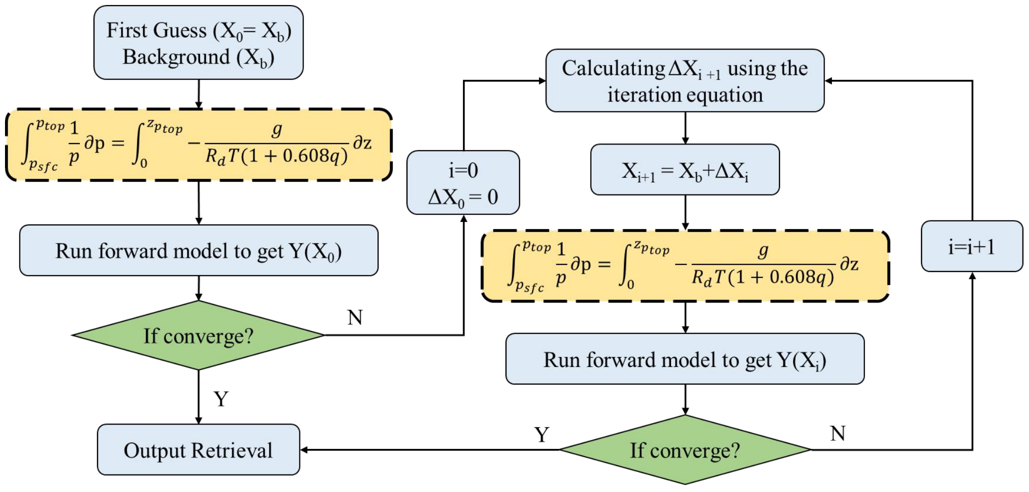


| EXP. NAME | Description |
|---|---|
| EXP_ctrl | Psfc directly retrieved based on background covariance. |
| EXP_hs | Psfc retrieved based on 1DVAR iteration coupled with hydrostatic balance. |

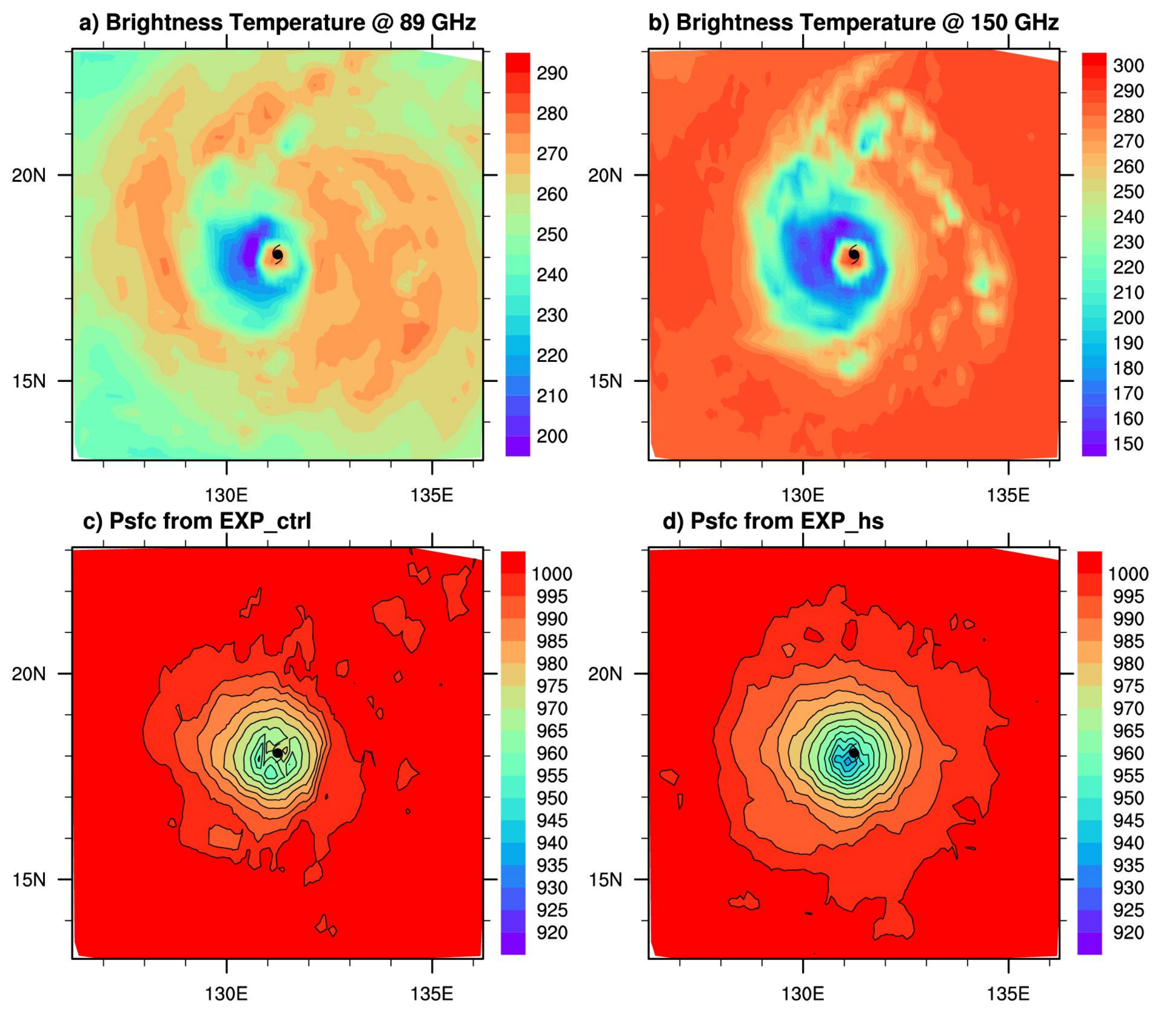

# 风云卫星微波全球大气温湿度反演精度

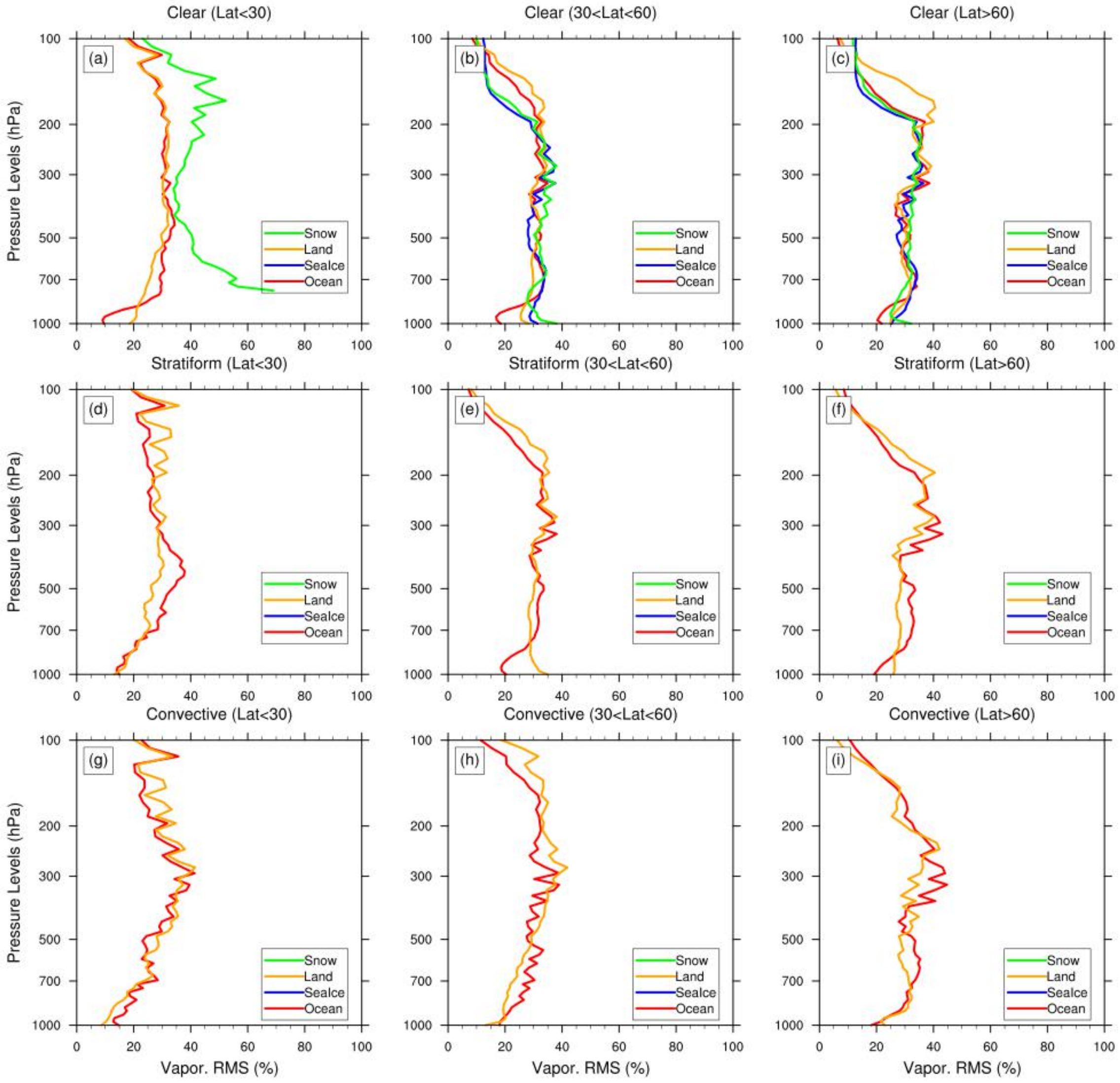


湿度廓线反演误差（RMS）

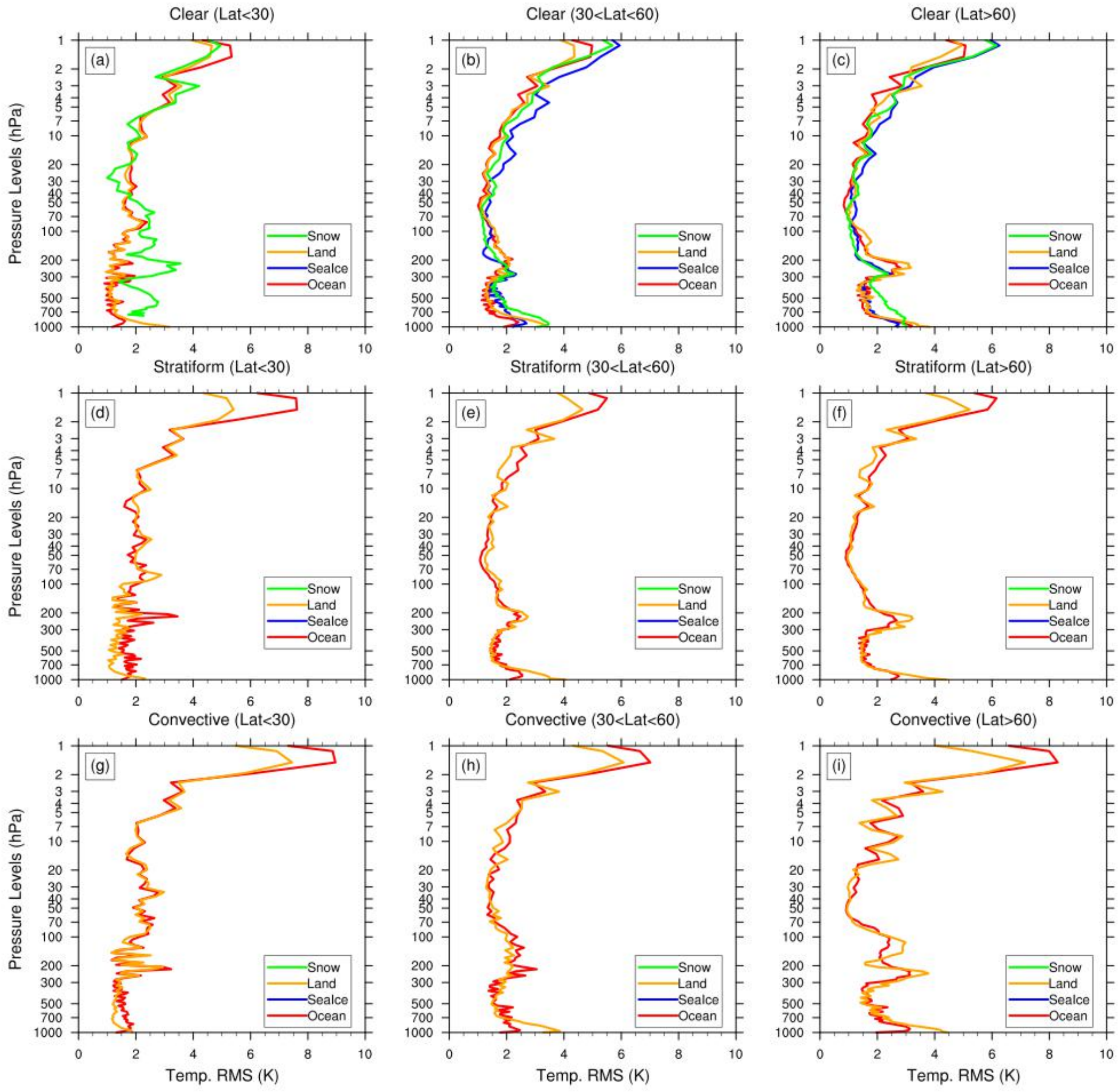


温度廓线反演误差（RMS）

# NOAA/CMA 微波大气温湿度反演精度比较

**CMWS vs ATMS**

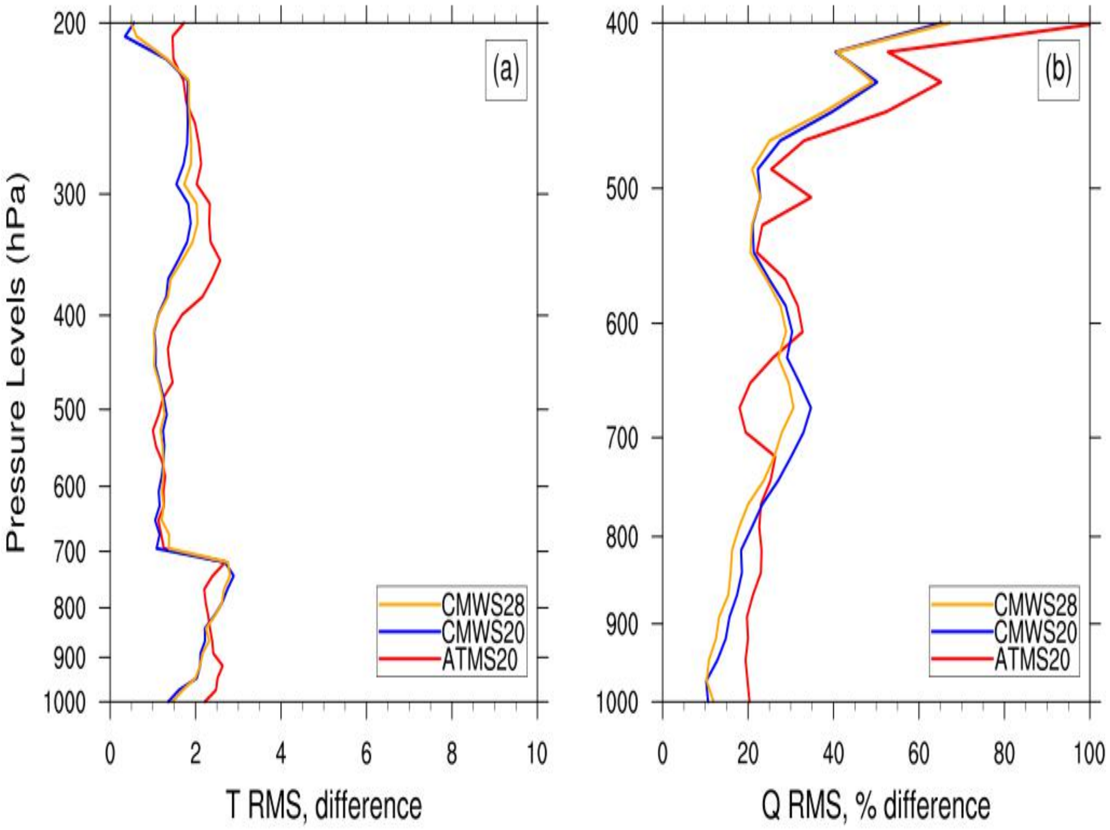


**MIRS vs GSDART**

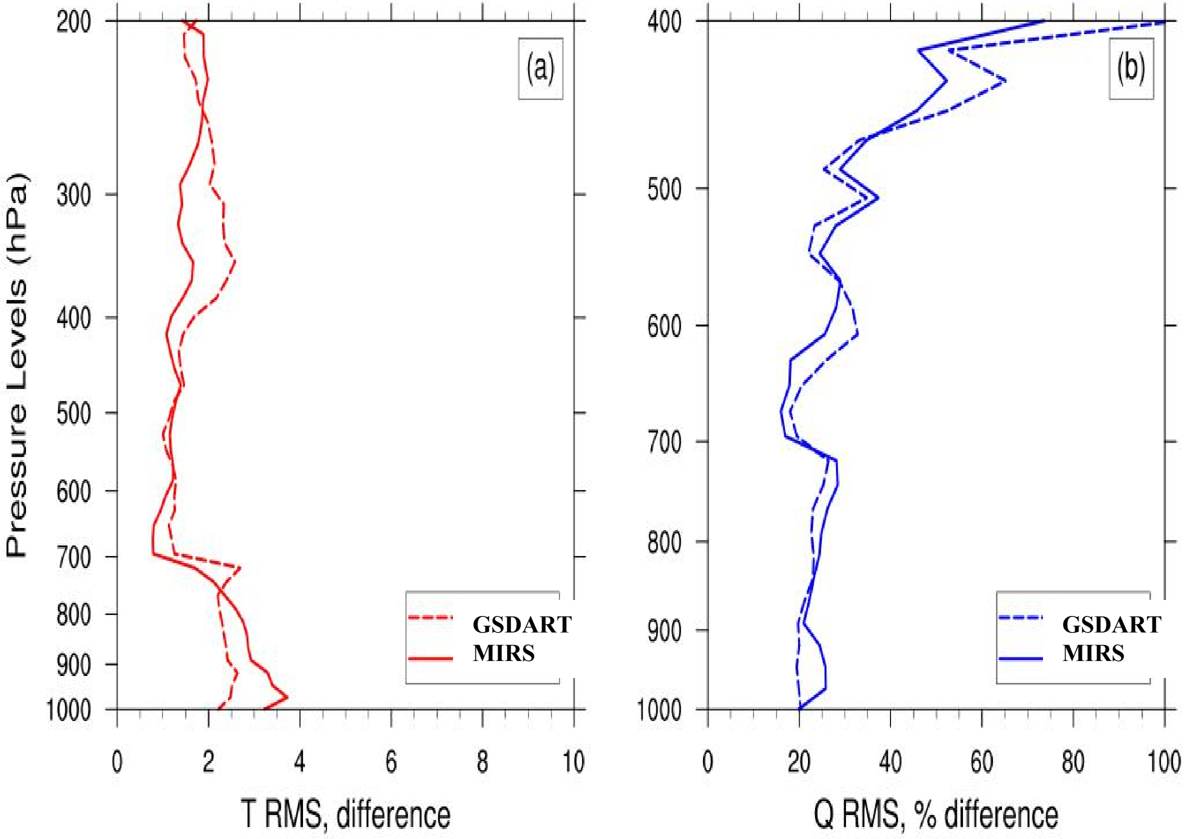


CMA CMWS has a better performance than NOAA ATMS

CMA GSDART has a better performance than NOAA-MIRS

# NOAA ATMS 和 FY-3D CMWS 暖核结果的比较

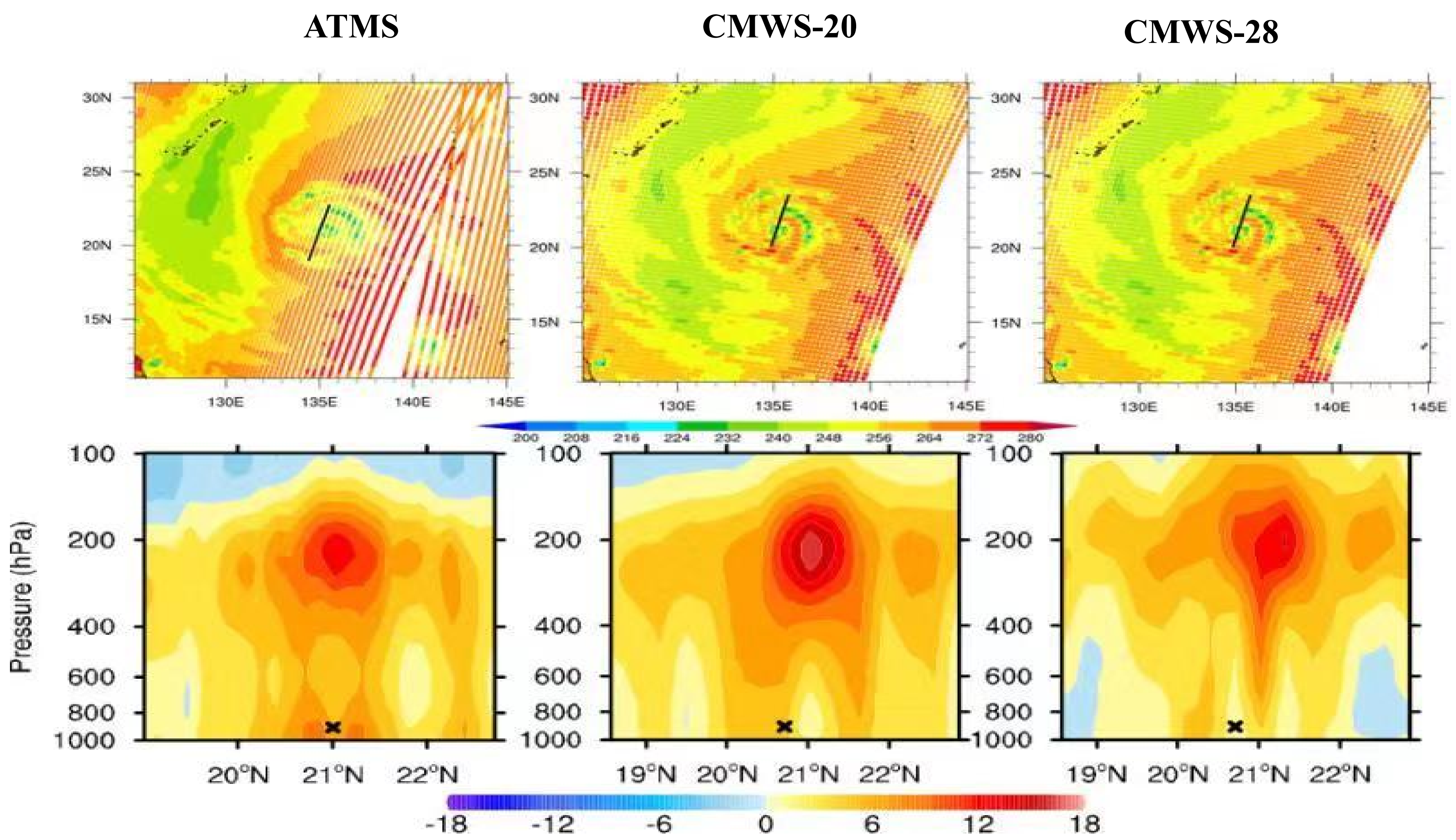

# 台风玛利亚（Maria）和山竹（Mangkhut）反演降水
# from FY-3 MWTS and MWHS

**Precipitation from CMWS-28**

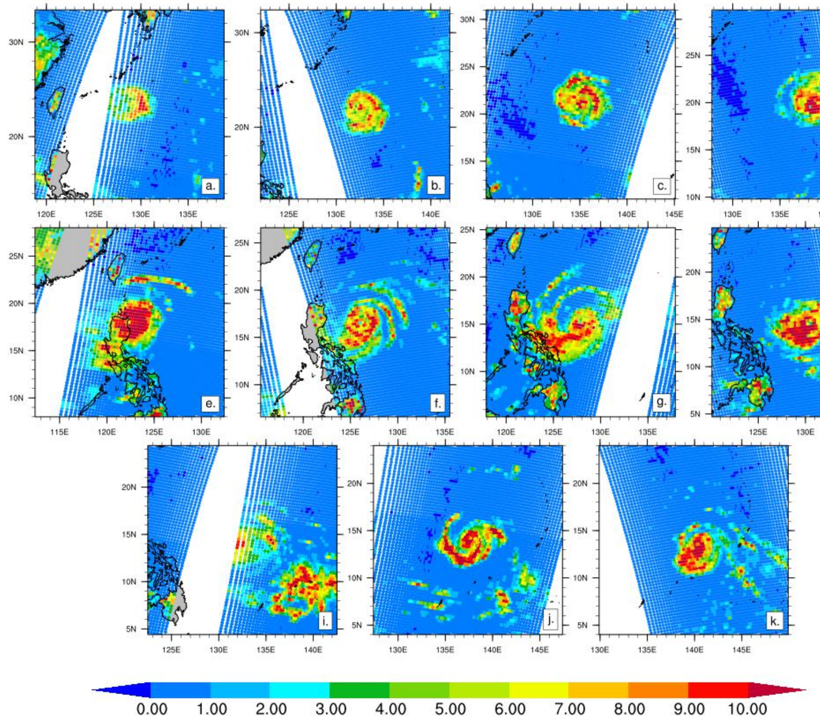


**Precipitation from CMORPH**

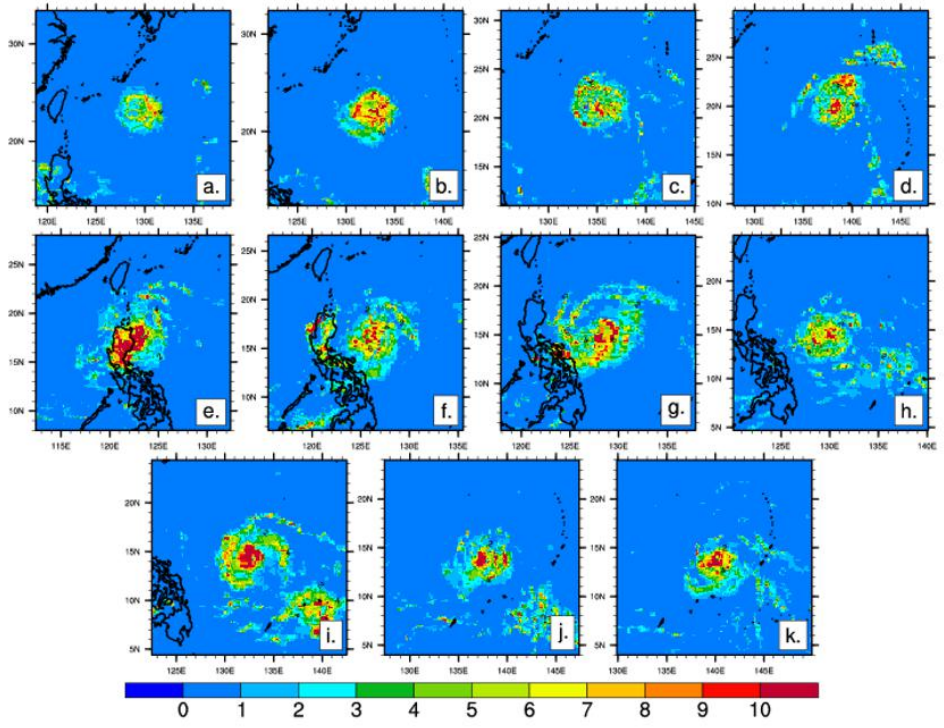


CMWS-28 is combined from MWTS and MWHS
CMORPH is NOAA multisensor precipitation products.

# 耦合静力积分反演海平面气压

| EXP. NAME | Description |
|---|---|
| EXP_ctrl | Psfc directly retrieved based on background covariance. |
| EXP_hs | Psfc retrieved based on 1DVAR iteration coupled with hydrostatic balance. |

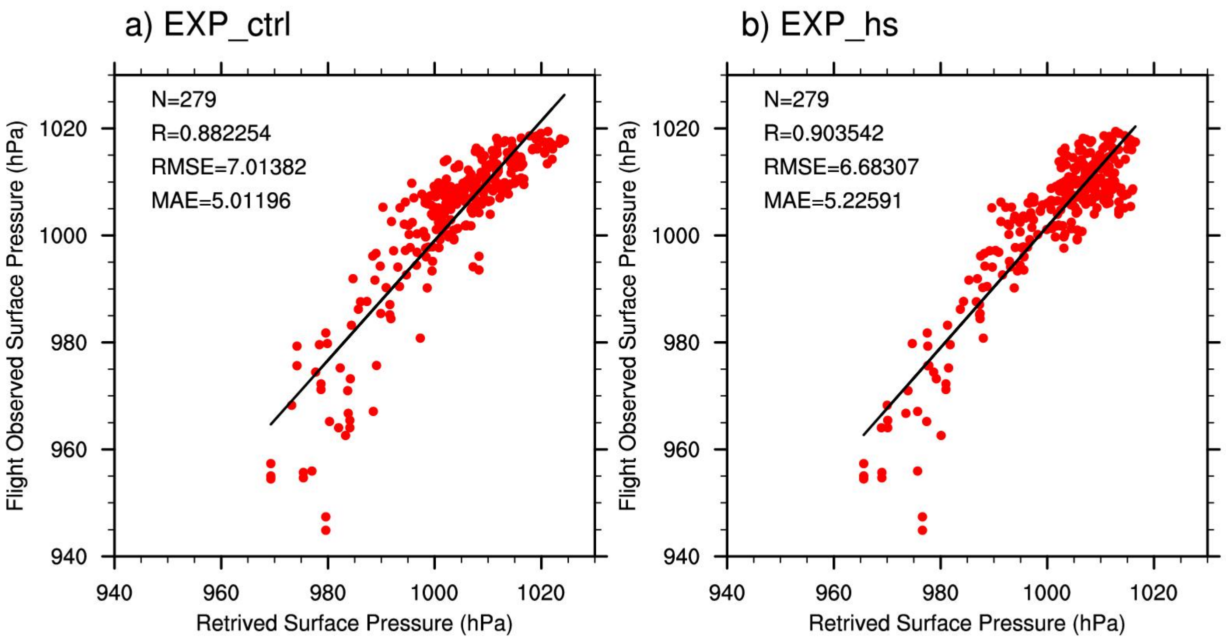


选取2018-2019大西洋海域和东太平洋海域飞机观测进行精度验证。
耦合静力平衡方程后，反演得到的海平面气压场RMSE可以达到6.68 hPa。
强台风由于气压梯度大，因此33km分辨率的微波探测仪观测资料对强台风的中心气压反演能力较差。

# 耦合静力积分反演海平面气压

WNP CMA

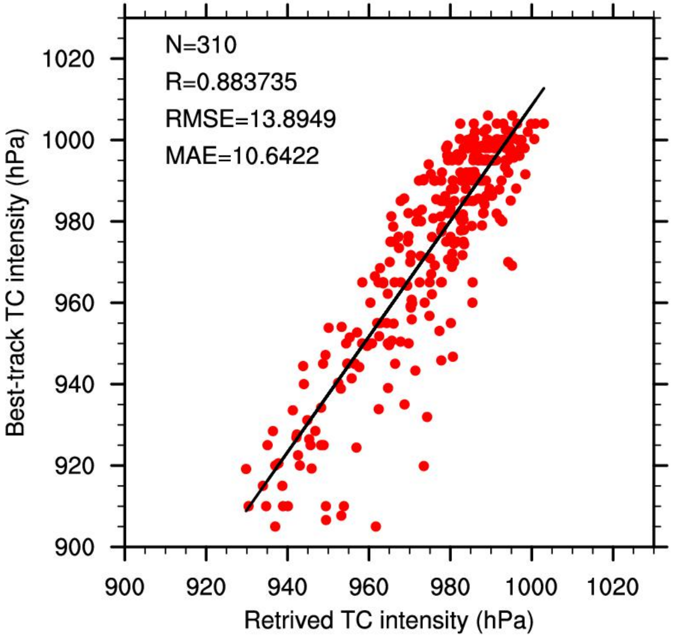


EP+ATL NHC

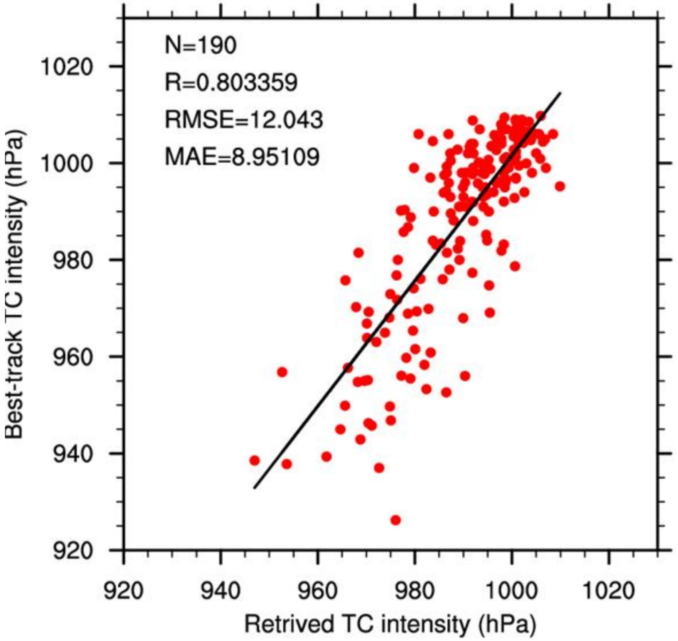


对比不同海域的定强结果可以看出，东太平洋和大西洋海域（12.04 hPa）的定强精度要优于西北太平洋海域（13.89 hPa），但是西北太平洋海域相关系数更高。

这可能与不同机构的定强算法差异有关。并且西北太平洋海域TC强度更强，会给粗分辨率的微波探测仪定强带来更大挑战。

# 风云卫星FY-3E(黎明星)微波大气探测郑州7-20特大洪水及台风“烟花”强度

FY-3E微波探测仪新增23.8 GHz和31.4 GHz两个低频窗区探测通道，对大气散射过程以及云和水汽的辐射较为敏感，为提高大气热力结构以及水凝物结构反演精度提供了重要观测信息。

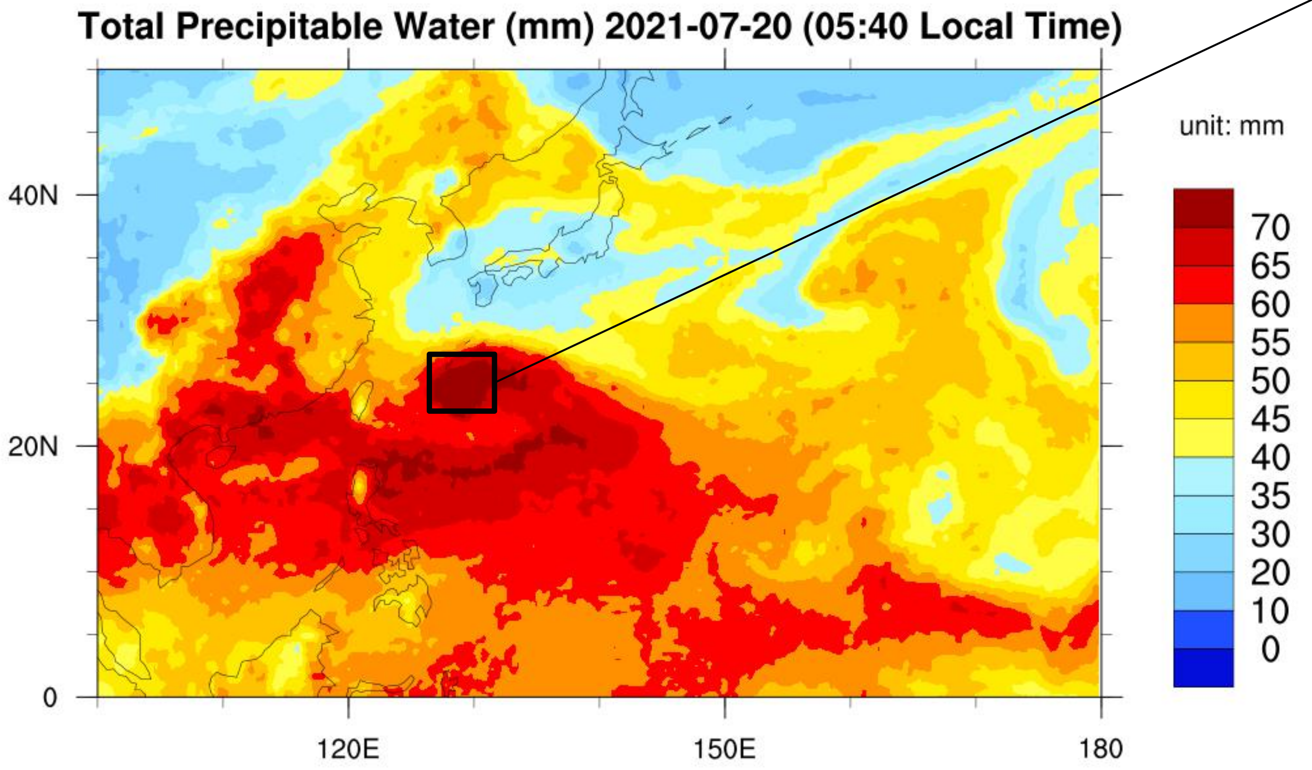


FY-3E微波融合大气可降水产品（TPW）指示了大气整层水汽含量分布情况。根据2021年7月20日FY-3E微波融合大气可降水产品（TPW）可以明显看出台风“烟花”环流区域的TPW高值区，河南附近与郑州暴雨过程相对应的TPW高值区，以及台风“烟花”向河南附近的水汽输送带。另外台风“烟花”北侧与副高相对应的TPW低值区也清晰可见。

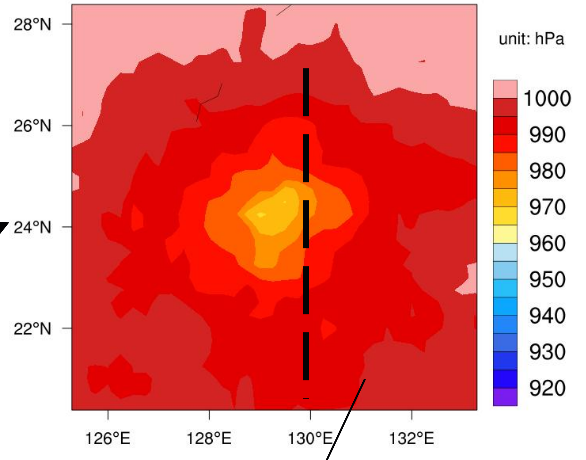


FY-3E微波融合海平面气压产品可以对台风尺度以及位置、强度进行监测。

根据FY-3E微波融合海平面气压产品可以看出台风“烟花” 海平面气压最低值大约为970 hPa，此时中央气象台的定强结果为975 hPa，这与我们海平面气压产品的最小值基本一致。

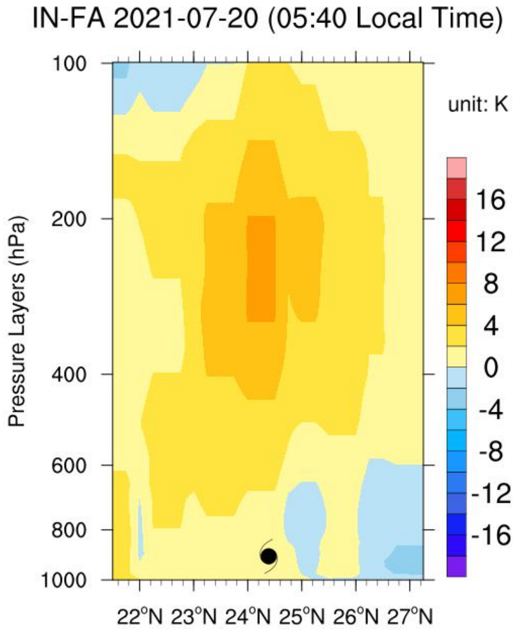


暖心结构产品是台风预报和监测最重要的产品之一，对台风结构、强度以及未来发展预测都有指示意义。

根据FY-3E微波融合台风暖心监测产品可以看出台风“烟花”的暖心高度大约位于300-200 hPa之间，暖心强度大约为6-8 K。

胡皓， 2021

# 风云卫星FY-3E(黎明星)微波大气探测产品保障全运会

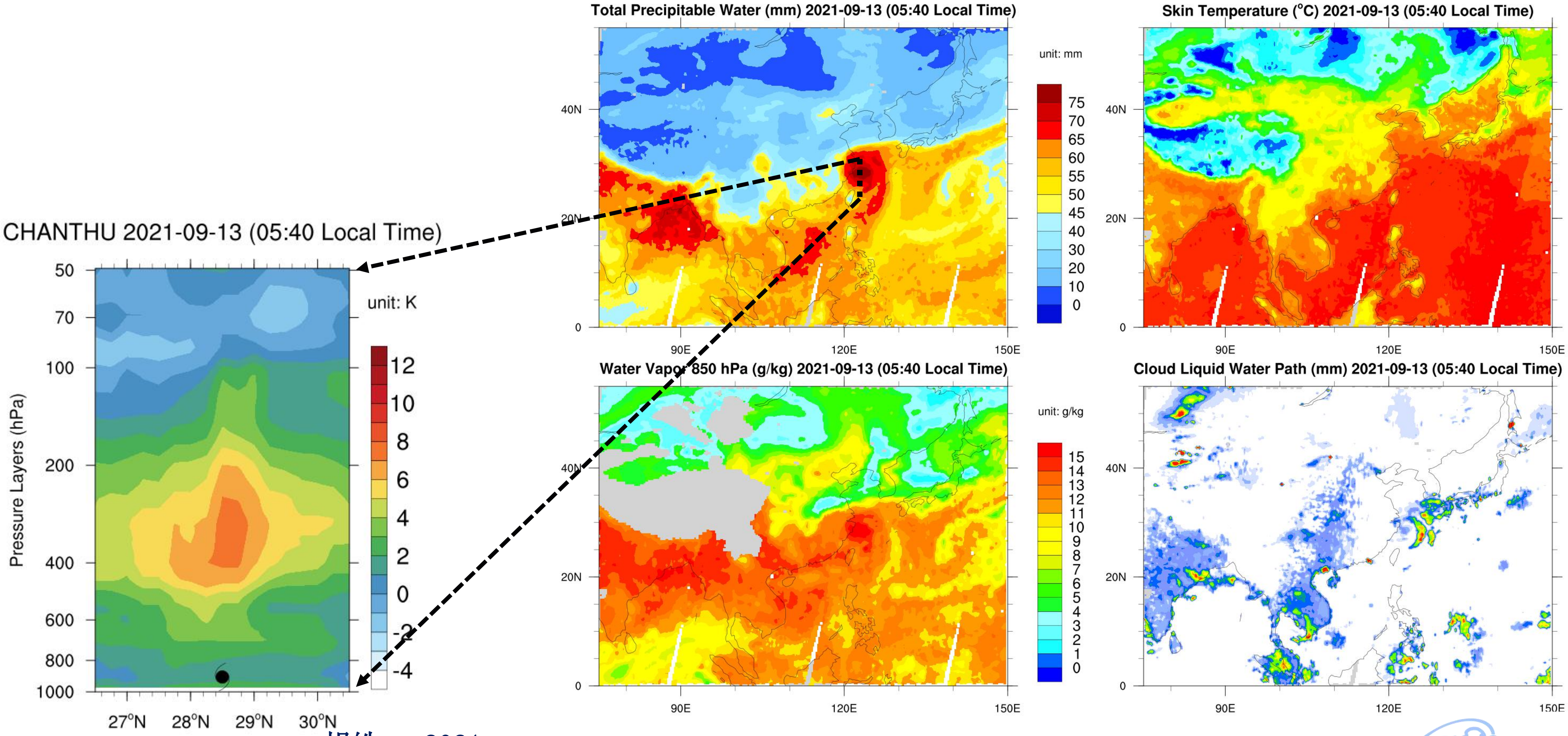


胡皓， 2021

# 风云卫星红外高光谱探测大气温湿反演和对流潜势监测

发挥卫星红外高光谱优势，开展影响大气温湿度反演关键技术研究，并逐步建立对流潜势监测模型

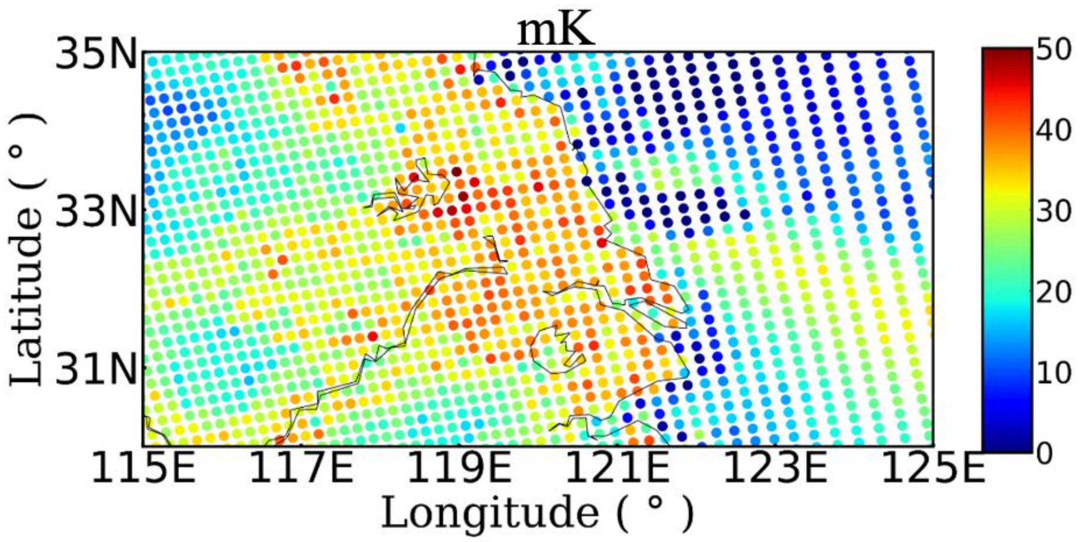


天气诊断指数—修正K指数

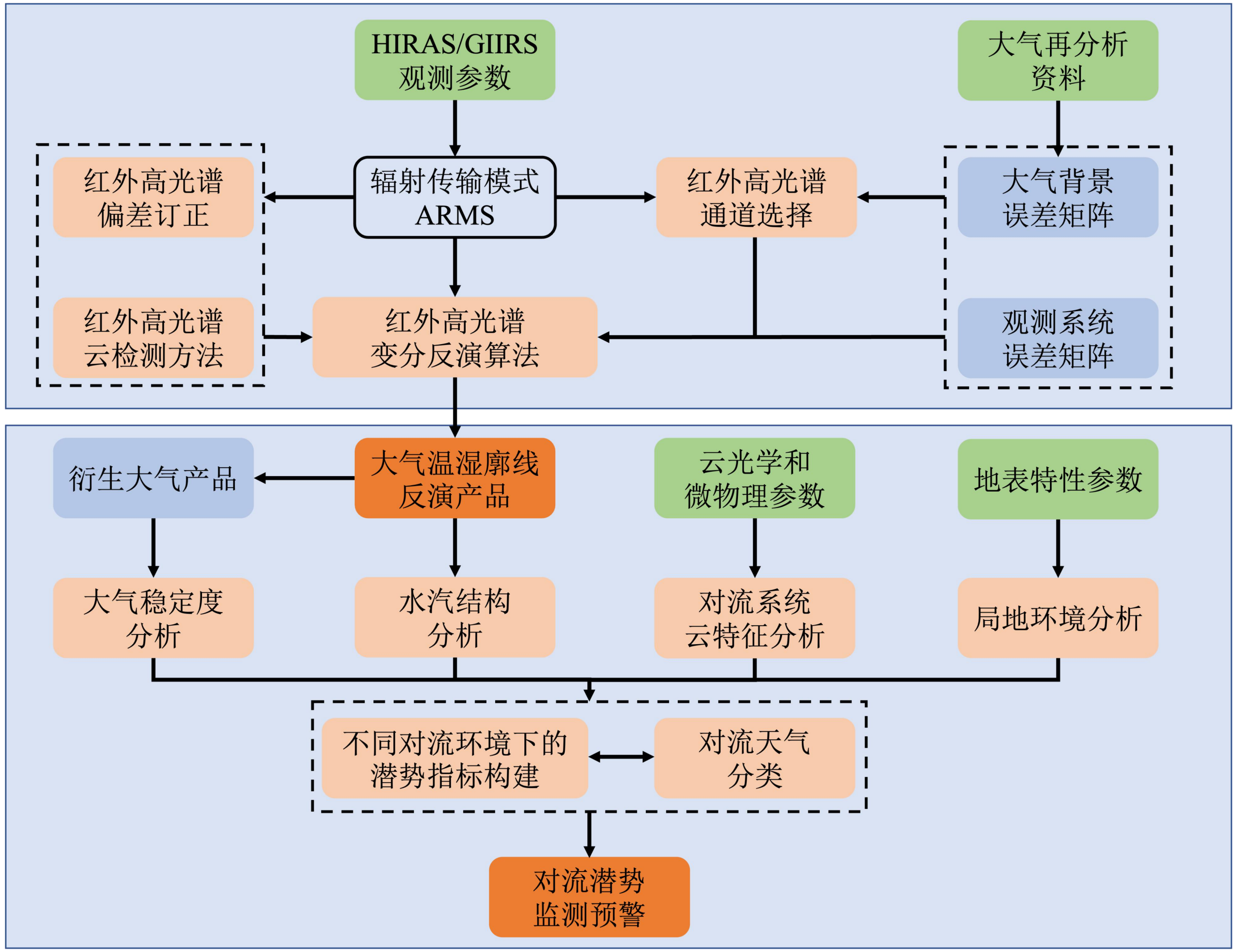


基于风云卫星红外高光谱对流潜势监测流程

姚彬，2022

# 风云卫星 FY-3D HIRAS-1 大气温湿度反演

- 进一步完善了风云卫星红外高光谱云检测和通道选择方案
- 建立起针对风云卫星红外高光谱探测统一的大气温湿度反演系统
- 开展洋面晴空大气下的反演，并进行算法精度评估与优化

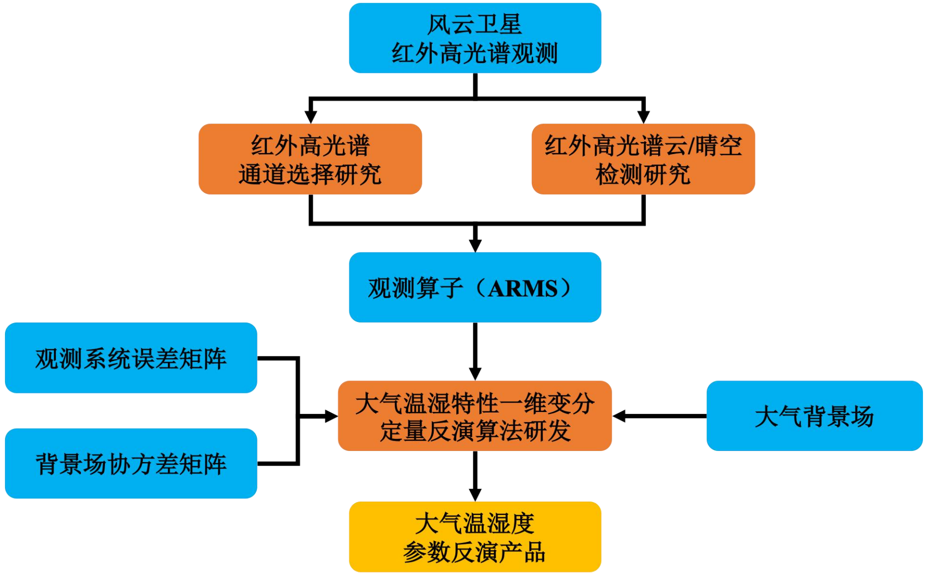


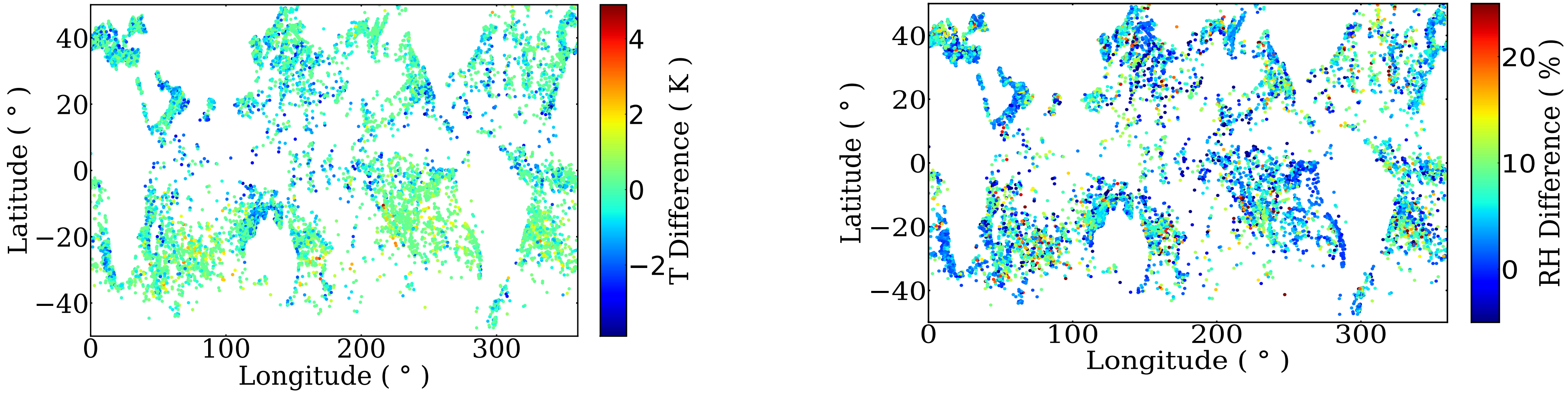


洋面温湿度反演偏差的空间分布（850 hPa）

姚彬，2021

# 风云卫星 FY-3D HIRAS-1 云/晴空检测

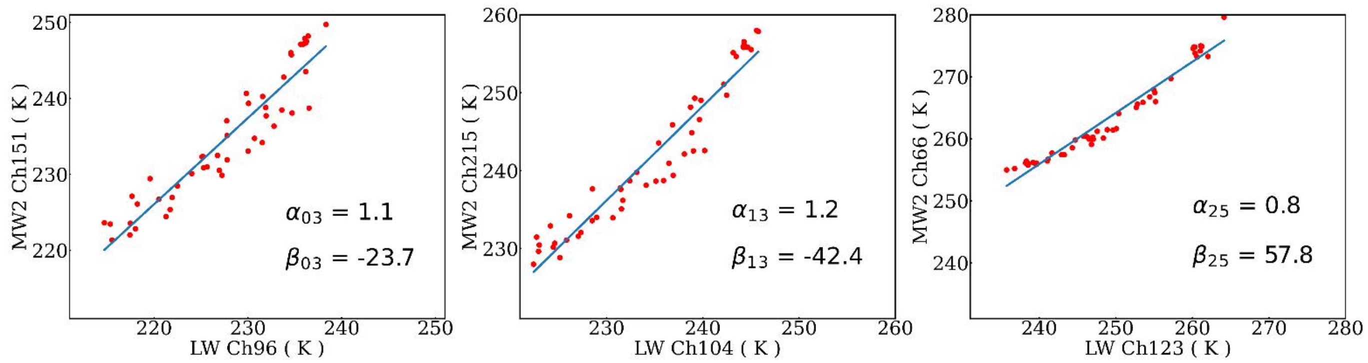


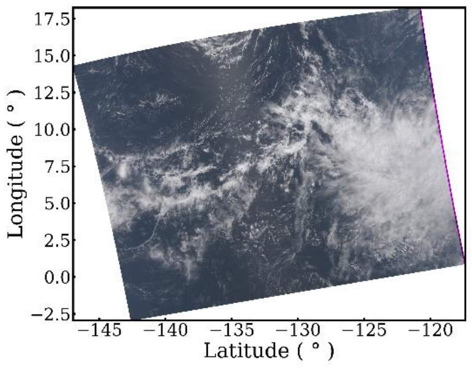


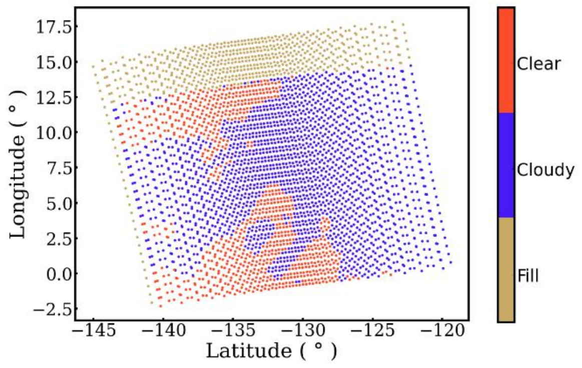


- 基于该方法能够有效识别出晴空/云像元；
- 整体结果与MODIS二级产品接近；
- 有待进一步评估性能，优化提高算法精度。

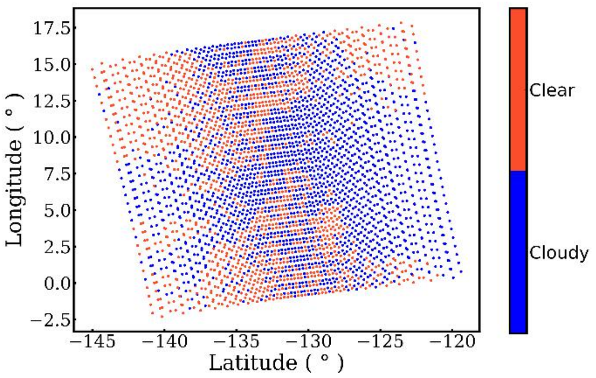


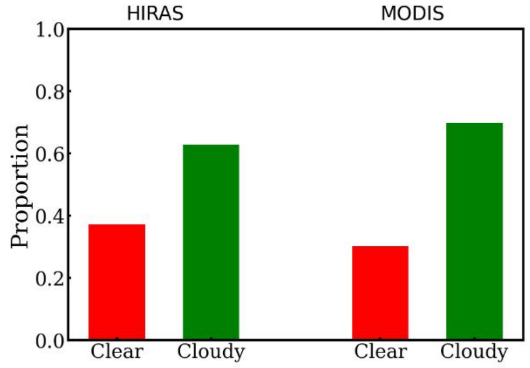


基于Double $CO_2$的红外高光谱云检测算法结果示意图，其中左上为同平台MERSI-II RGB图，左下为本算法云检测结果，右上为MODIS结果，右下为定量对比情况

姚彬，2022

当前该算法为基于HIRAS/FY3D观测

# 风云卫星 FY-3E HIRAS-2 Mean O-B

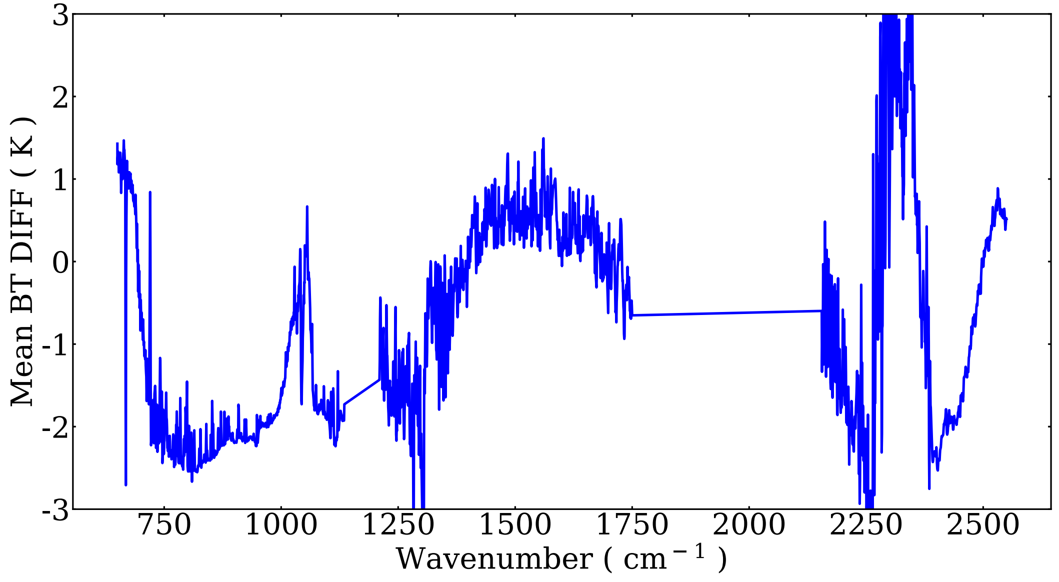


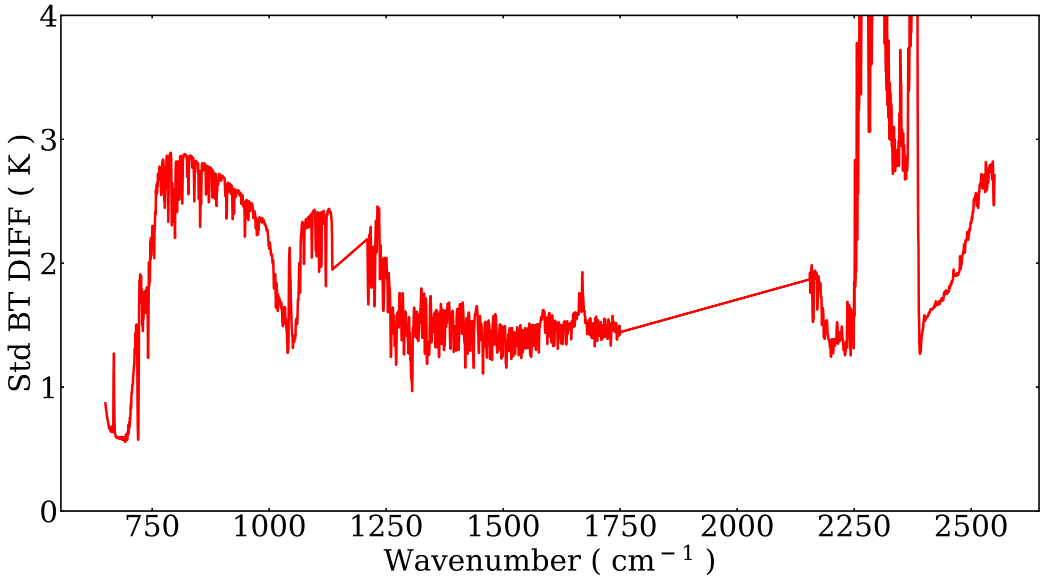


基于HIRAS-II/FY3E的模拟与观测相比的亮温差平均值（左图）和标准差（右图）情况
（所选用数据为2021.12.10 - 2021.12.20共计约7万个海上晴空像素点，云检测为基于Double $CO_2$的检测方法，模拟所用大气廓线为ERA5再分析资料）

**LW平均偏差1.5 K, MW1平均偏差0.2 K, MW2平均偏差0.5 K**

**需要注意的是：当前HIRAS-II/FY3E的系数文件中的通道设置与HIRAS/FY3D的系数文件中通道设置类似，因此只有图示2275个通道模拟结果**

姚彬，2022

# 风云卫星 FY-3E HIRAS-2 FOV 依赖 的O-B分布

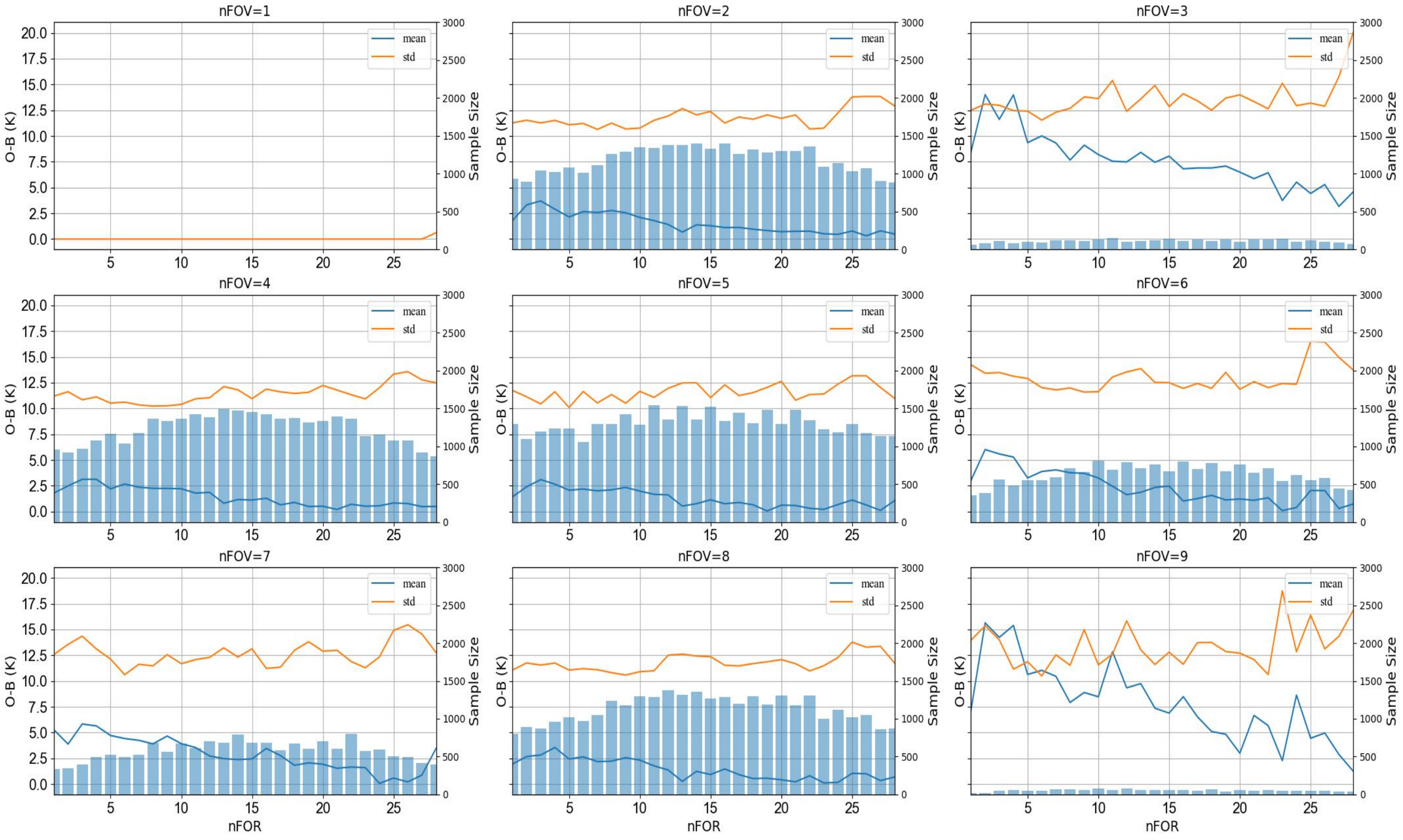


wave_length=11.63$\mu m$

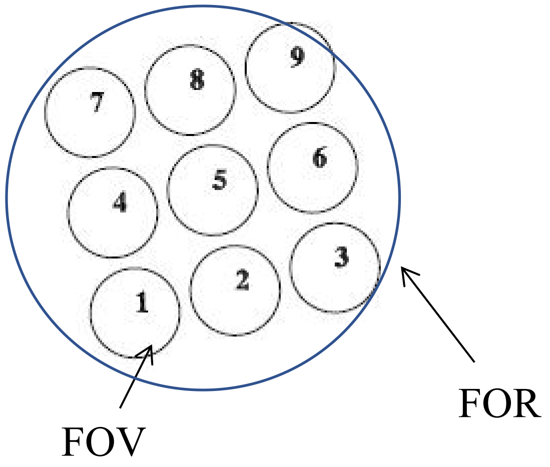


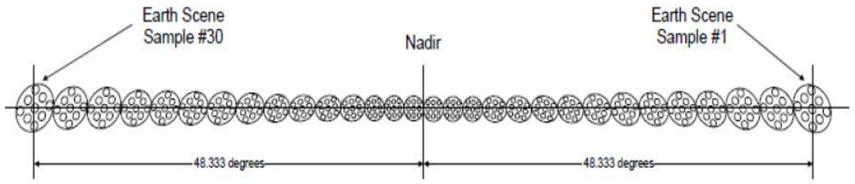


方程格格，2022

# FY-3E GNOS-R 海面风速反演基本原理

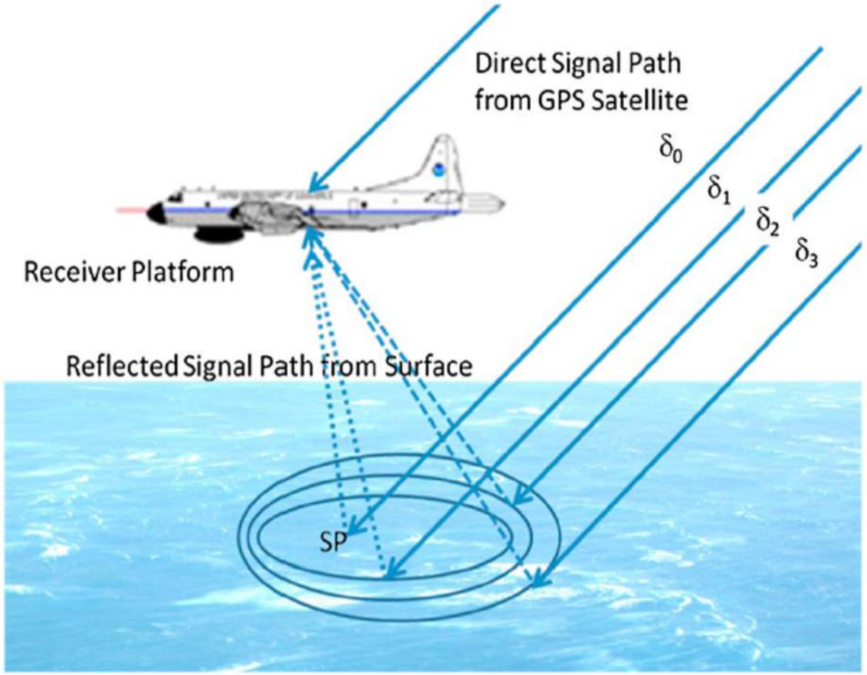


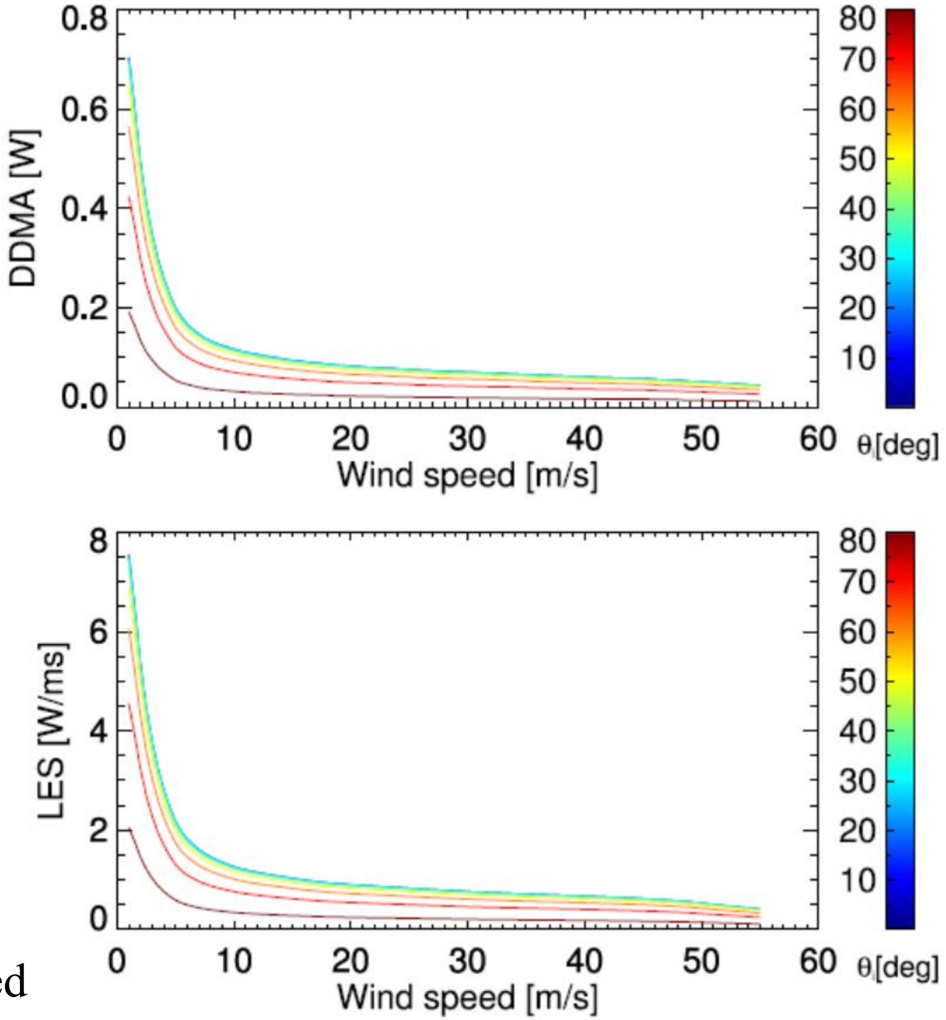


The DDMA represents an average of a Doppler Delay Map (DDM) over a given delay/Doppler range window around the specular point

The LES refers to the slope of the leading edge of the integrated delay waveform

$$U_{10}^{MV} = k_0 | U_{10}^{DDMA} + k_1 U_{10}^{LES}$$

Paul Chang, NOAA, 2016

# FY-3E WindRad 和 GNOS-R 正向模式算法

## Two-Scale Roughness Model for Polarimetric BRDF Simulation

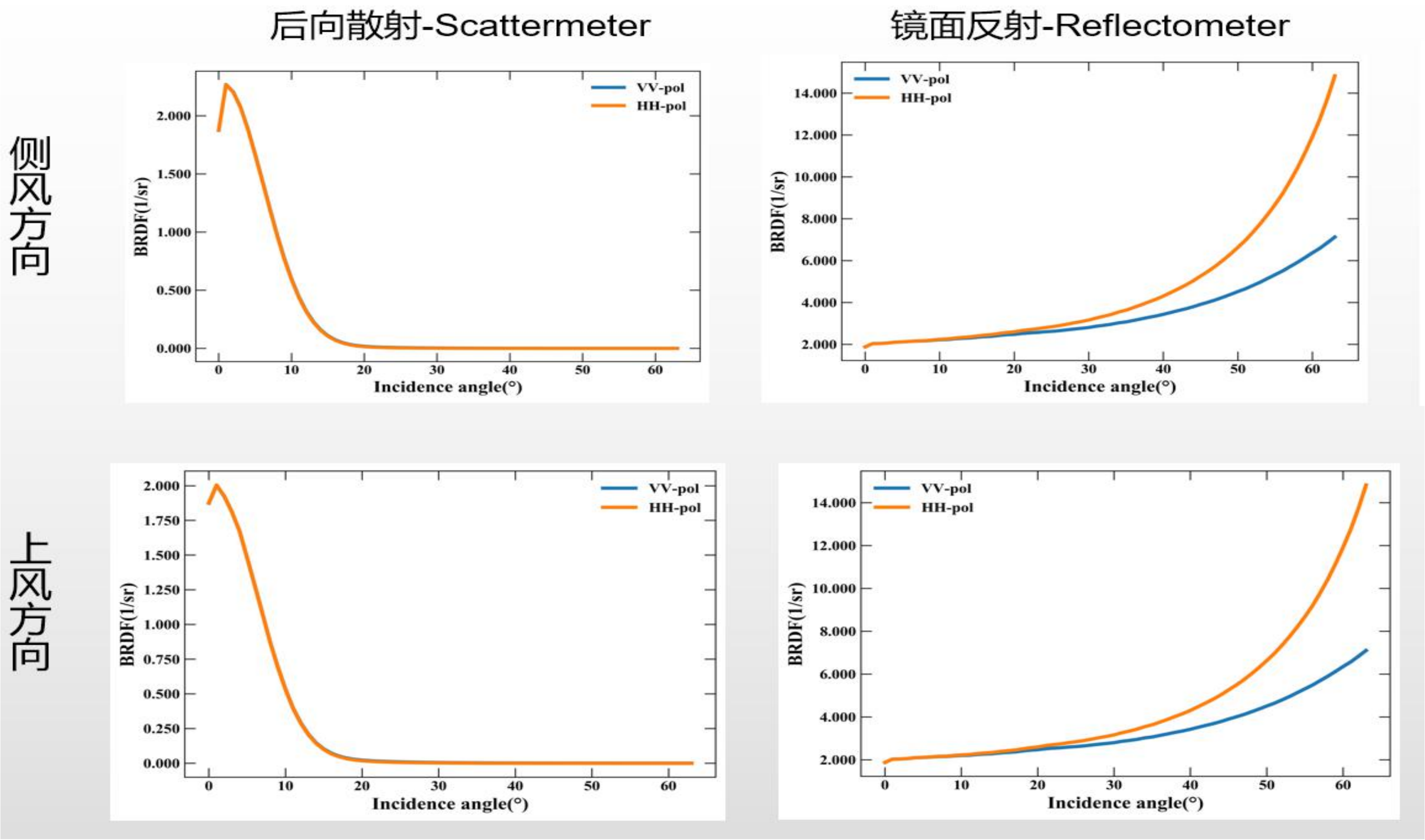


何灵利， 2022

# FY-3E GNSS-R海面风速资料前处理中质量控制

| 质量控制方法 | GPS数据剔除比例 | BDS数据剔除比例 |
|---|---|---|
| RCG>15 | 29.8% | 41.5% |
| DDMA风速与LES风速相差过大 | 18.5% | 23.8% |
| 其他 | 2.7% | 2.9% |
| 合计（包含于质量标识符） | 42.3% | 53.4% |

RCG = range corrected gain

DDMA = delay-Doppler map average

LES = leading edge slope

$$RCG = \frac{G_{Rx}^{Sp}}{(R_{TxSp} R_{RxSp})^2}$$

**Quality control: RCG > 25, wind speed < 25 m/s**

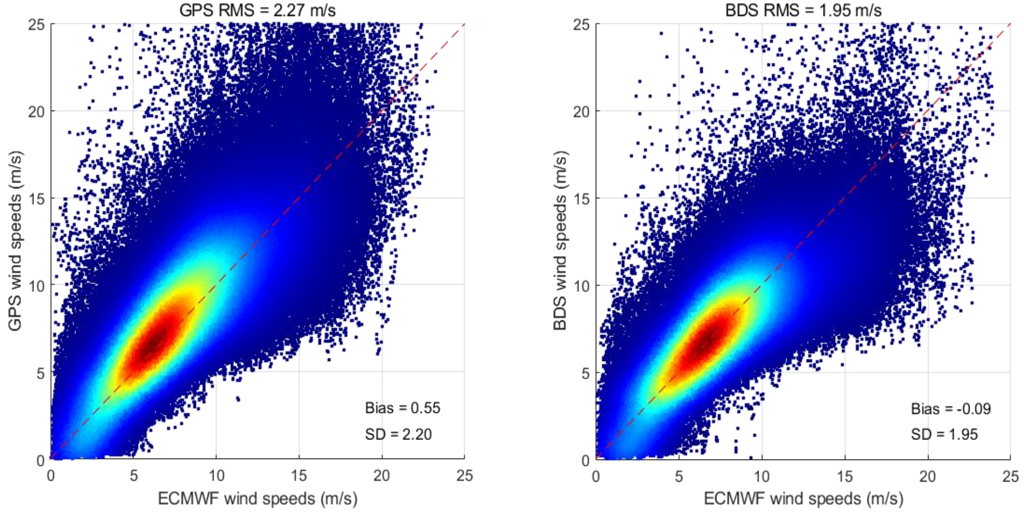


刘艳，2021

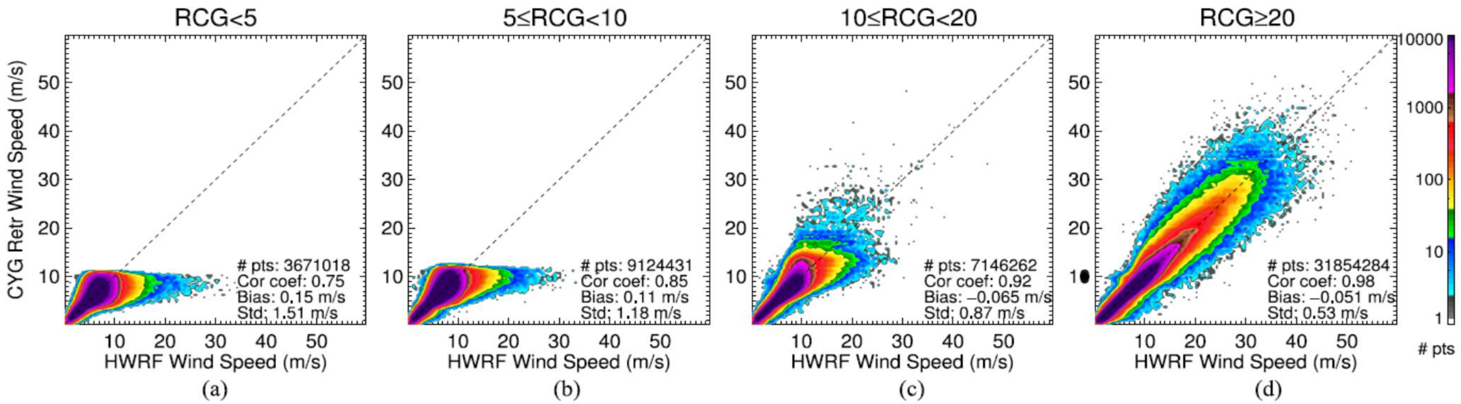


Said et al, 2016; JSTARS

# FY3E的GNSS-R反射计风速与METOP和CYGNSS风速的比较

GNOS GNSS-R WIND SPEED

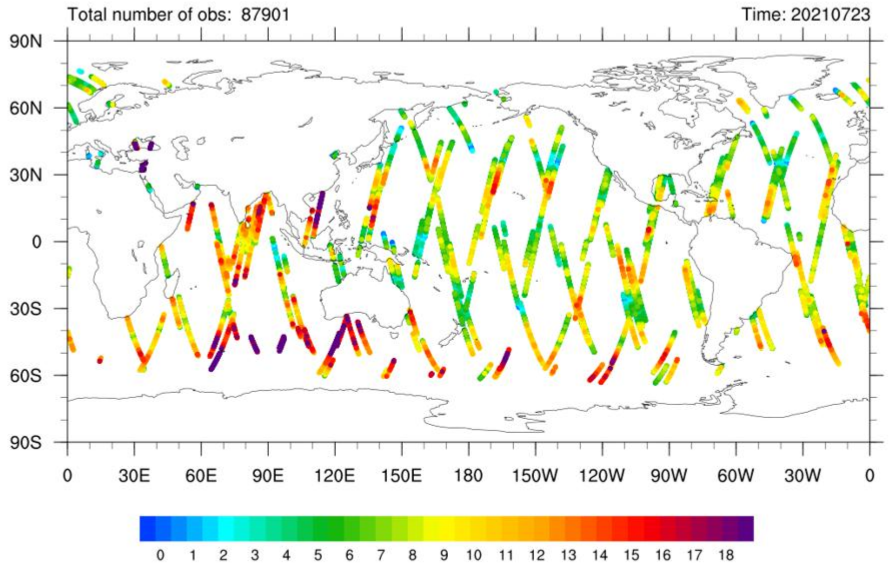


SCAT WIND SPEED

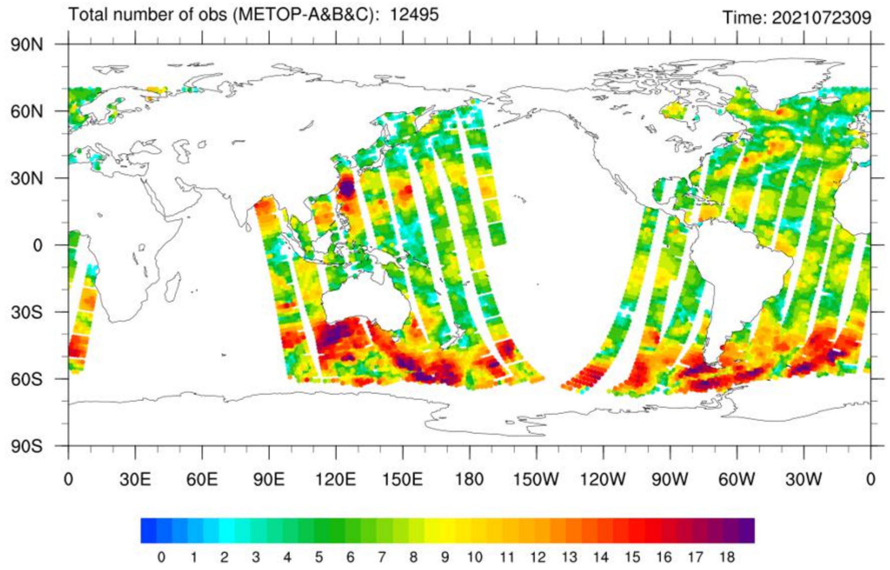


CYGNSS WIND SPEED

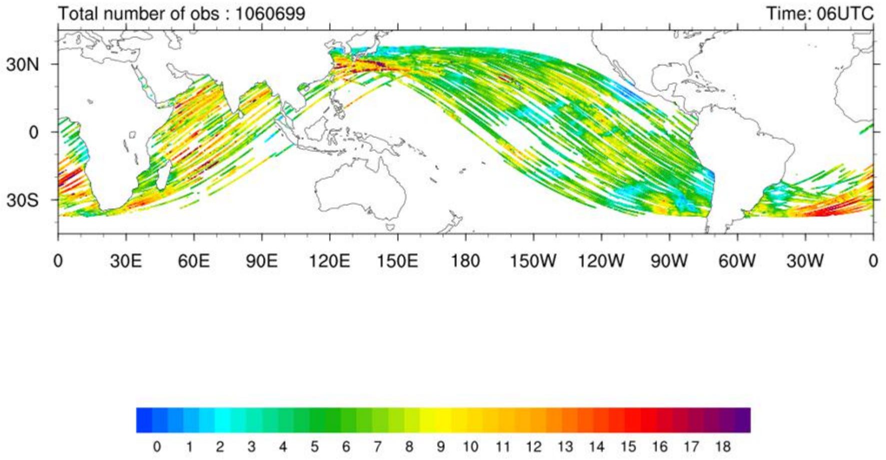


刘艳，2021

# Summary and Conclusions

- CMA Earth System Modeling and Prediction Center (**CEMC**) is fully prepared for uses of FY-3E data in its data assimilation systems. The forward operators (**ARMS** and **RTTOV**) are fully ready for CMA data assimilation and other applications.
- Initial checks of L1 data from FY-3E MWTS-3, MWHS-2, HIRAS-2 are completed. The polarization alignment of two newly-added **K/Ka** bands in MWTS-3 is characterized as **quasi-horizontal (QH)** for the best simulation. These two bands are critical for quality control in NWP data assimilation system.
- FY-3E HIRAS-2 O-B is being analyzed and is well behaved in terms of the band mean errors and **FOV-dependent** values.
- In 2021, FY-3E MWTS/MWHS data were also utilized to support the **major national events** and the products were used for the major briefing as required according to CMA in-orbit calibration guidance.
- Finally, we would like to express our gratitude to FY-3E calval team for their ***professional*** and ***diligent*** works and timely share the data with user community. It is your open-data policy that will prosper this great nation's FY-3 mission.